

# NAVAL POSTGRADUATE SCHOOL MONTEREY, CALIFORNIA



## THESIS

### VERTICAL PROFILES OF LONGSHORE CURRENTS

by

Carlos Manuel da Costa Ventura Soares

September, 1995

Thesis Advisor:

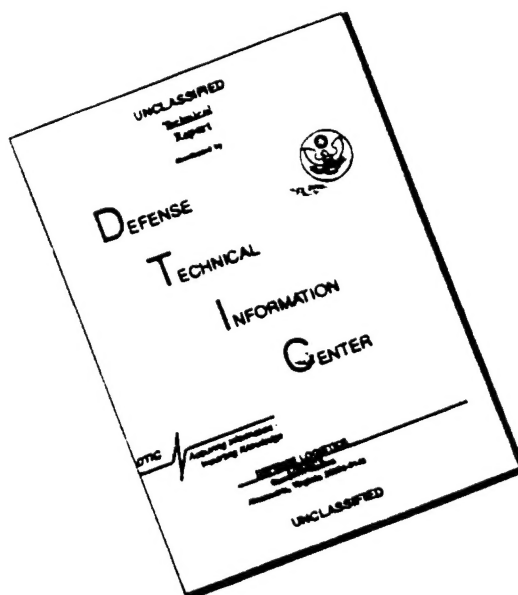
Edward B. Thornton

Approved for public release; distribution is unlimited.

19960315 051

DTIC QUALITY INSPECTED 1

# DISCLAIMER NOTICE



THIS DOCUMENT IS BEST QUALITY AVAILABLE. THE COPY FURNISHED TO DTIC CONTAINED A SIGNIFICANT NUMBER OF PAGES WHICH DO NOT REPRODUCE LEGIBLY.

REPORT DOCUMENTATION PAGE			Form Approved OMB No. 0704-0188	
Public reporting burden for this collection of information is estimated to average 1 hour per response, including the time for reviewing instruction, searching existing data sources, gathering and maintaining the data needed, and completing and reviewing the collection of information. Send comments regarding this burden estimate or any other aspect of this collection of information, including suggestions for reducing this burden, to Washington Headquarters Services, Directorate for Information Operations and Reports, 1215 Jefferson Davis Highway, Suite 1204, Arlington, VA 22202-4302, and to the Office of Management and Budget, Paperwork Reduction Project (0704-0188) Washington DC 20503.				
1. AGENCY USE ONLY (Leave blank)		2. REPORT DATE September 1995		3. REPORT TYPE AND DATES COVERED Master's Thesis
4. TITLE AND SUBTITLE VERTICAL PROFILES OF LONGSHORE CURRENTS			5. FUNDING NUMBERS	
6. AUTHOR(S) Soares, Carlos, V.				
7. PERFORMING ORGANIZATION NAME(S) AND ADDRESS(ES) Naval Postgraduate School Monterey CA 93943-5000			8. PERFORMING ORGANIZATION REPORT NUMBER	
9. SPONSORING/MONITORING AGENCY NAME(S) AND ADDRESS(ES)			10. SPONSORING/MONITORING AGENCY REPORT NUMBER	
11. SUPPLEMENTARY NOTES The views expressed in this thesis are those of the author and do not reflect the official policy or position of the Department of Defense or the U.S. Government.				
12a. DISTRIBUTION/AVAILABILITY STATEMENT Approved for public release; distribution is unlimited.			12b. DISTRIBUTION CODE	
13. ABSTRACT (maximum 200 words) <p>The vertical structure of the mean longshore current is examined on three strong current days during the DUCK94 experiment and it is found well described by a logarithmic profile (mean correlation coefficient for all 22 profiles, 0.98). This hypothesis works better in the trough where turbulent bottom boundary layer processes are predominant than over the bar, where breaking-wave induced turbulence generated at the surface modifies the profile.</p> <p>A relationship between near bottom vertical velocity profiles and bottom roughness was found. The bed shear stress coefficient varied by an order of magnitude across the surf zone (0.001-0.05). For the three days considered, it is concluded that the bed shear stress coefficient increased with increasing bottom roughness, and therefore is an important parameter to characterize the bottom boundary layer.</p> <p>The influence of the wind is parameterized by an exponential approximation that works well in 50% of the analyzed profiles. This parameterization assumes that the residual Data-Normal distribution of data is only due to the wind and does not consider the alongshore component of mass transport velocity, which is assumed small.</p> <p>These results should be treated carefully since there were obtained for only three days over a barred beach with strong longshore currents, and cannot be generalized without further studies.</p>				
14. SUBJECT TERMS Nearshore; Longshore currents; Boundary layer.			15. NUMBER OF PAGES 80	
			16. PRICE CODE	
17. SECURITY CLASSIFICATION OF REPORT Unclassified	18. SECURITY CLASSIFICATION OF THIS PAGE Unclassified	19. SECURITY CLASSIFICATION OF ABSTRACT Unclassified	20. LIMITATION OF ABSTRACT UL	



Approved for public release; distribution is unlimited

**VERTICAL PROFILES  
OF  
LONGSHORE CURRENTS**

Carlos Manuel da Costa Ventura Soares  
Lieutenant , Portuguese Navy  
B.S., Portuguese Naval Academy, 1986

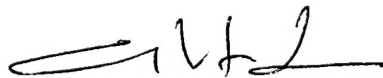
Submitted in partial fulfillment  
of the requirements for the degree of

**MASTER OF SCIENCE IN PHYSICAL OCEANOGRAPHY**

from the

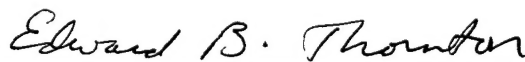
**NAVAL POSTGRADUATE SCHOOL  
September 1995**

Author:



Carlos Manuel da Costa Ventura Soares

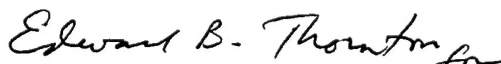
Approved by:



Edward B. Thornton, Thesis Advisor



Timothy P. Stanton, Second Reader



Robert Bourke, Chairman  
Department of Oceanography



## ABSTRACT

The vertical structure of the mean longshore current is examined on three strong current days during the DUCK94 experiment and it is found well described by a logarithmic profile (mean correlation coefficient for all 22 profiles, 0.98). This hypothesis works better in the trough where turbulent bottom boundary layer processes are predominant than over the bar, where breaking-wave induced turbulence generated at the surface modifies the profile.

A relationship between near bottom vertical velocity profiles and bottom roughness was found. The bed shear stress coefficient varied by an order of magnitude across the surf zone (0.001-0.05). For the three days considered, it is concluded that the bed shear stress coefficient increased with increasing bottom roughness, and therefore is an important parameter to characterize the bottom boundary layer.

The influence of the wind is parameterized by an exponential approximation that works well in 50% of the analyzed profiles. This parameterization assumes that the residual Data-Normal distribution of data is only due to the wind and does not consider the alongshore component of mass transport velocity, which is assumed small.

These results should be treated carefully since there were obtained for only three days over a barred beach with strong longshore currents, and cannot be generalized without further studies.





## TABLE OF CONTENTS

I. INTRODUCTION .....	1
II. THEORY .....	5
A. BOTTOM BOUNDARY LAYER .....	5
B. SURFACE BOUNDARY LAYER .....	8
III. DUCK 94 EXPERIMENT .....	15
IV. DATA RESULTS .....	19
V. DISCUSSION .....	25
VI. CONCLUSIONS .....	29
APPENDIX A. FIGURES .....	31
APPENDIX B. TABLES .....	57
LIST OF REFERENCES .....	61
INITIAL DISTRIBUTION LIST .....	63



## LIST OF FIGURES

1. SLED on the Beach During DUCK94 Experiment..	33
2. Bathymetry and Equipment Positioning During DUCK94 Experiment (11 Oct.).	
Sled Transect Line was 940 m Alongshore .....	34
3. Bathymetry Profiles for the Three Days Considered (10, 11 and 12 Oct.)..	35
4. Climatology for the Three Days Considered (10, 11 and 12 Oct.). Currents Were	
Measured in the Middle of the Trough. H is the Significant Wave Height and T is	
the Period of Peak Frequency .....	36
5. (a) Least-Squares Fit to the Data for 10 Oct. ....	37
5. (b) Least-Squares Fit to the Data for 11 Oct. ....	38
5. (c) Least-Squares Fit to the Data for 12 Oct. ....	39
6. Example of Vertical Profile (the Upper Two Current Meters Sometimes Were Out	
of the Water) .....	40
7. (a) Vertical Profiles of Mean Longshore Currents for 10 Oct. ....	41
7. (b) Vertical Profiles of Mean Longshore Currents for 11 Oct. ....	42
7. (c) Vertical Profiles of Mean Longshore Currents for 12 Oct. ....	43
8. Variation of the <i>Rms</i> Bottom Roughness with the Cross-Shore Distance .....	44
9. Relationship Between $c_f$ and $U_m / V$ .....	45
10. Relationship Between $\frac{z_a}{h}$ and $U_m / V$ .....	46

11. Bed Shear Stress versus Bottom Roughness. The Line Represents a Linear Regression Based on All Points but the Outlier . . . . .	47
12. $C_f$ versus $\frac{r}{A}$ . . . . .	48
13. $\frac{z_a}{h}$ versus $\frac{r}{A}$ (Outlier not Included). . . . .	49
14. $C_f$ versus Cross-Shore Distance . . . . .	50
15. $v_t$ versus Cross-Shore Distance . . . . .	51
16. Relationship Between $C_f$ and $\gamma$ . . . . .	52
17. Relationship Between $v_t$ and $\gamma$ . . . . .	53
18. Example of Wind Contribution to the Longshore Current: Exponential Approximation to the Residual . . . . .	54
19. Relationship Between $\frac{z_a}{h}$ and $\frac{H_{rms}}{h^{3/2}} \frac{r}{v_*}$ . . . . .	55

## LIST OF TABLES

1. Profile Fitting Results .....	59
2. Wind Data .....	60



## ACKNOWLEDGMENTS

The author wishes to express his appreciation to all those who participated in DUCK94 experiment, namely the staff of the U.S. Army Field Research Facility under the direction of B. Birkemeier. In addition, special appreciation is expressed to R. Wyland, Naval Postgraduate School for his role in acquisition of wave and current data, and to Mary Bristow, Naval Postgraduate School, for help in processing data. Thanks to LT Jeff Swayne, USN, for providing bottom roughness data. Finally a special thanks to Tom Lippmann, Naval Postgraduate School, to Timothy Stanton and Edward Thornton for their important suggestions and orientations.

Lastly and most importantly, I want to express my sincere thanks to my wife, Sonia. Without her love, support, encouragement and understanding, this thesis would never have been written.





## I. INTRODUCTION

Knowledge of the bottom and surface boundary layers is fundamental to understanding nearshore hydrodynamic and sediment processes. For steady flow, such as in a river, the bottom boundary layer is well described by a logarithmic profile. The superposition of waves on the mean current produces enhanced bottom friction (e.g., Grant and Madsen (1979), Christofferson and Jonsson (1985), Myrhaug and Slaattelid (1989) and Sleath (1990)). As a result, the gradient of mean current near the bed is decreased and a more linear profile can be expected. The influence by waves is inversely proportional to the depth of the water with decreasing importance of wave-bottom boundary with increasing depth.

Only limited wave-driven, longshore current vertical profiles have been measured. Visser (1984) measured wave-driven longshore currents in a laboratory experiment using dye displacement over the vertical. He found the alongshore spatially averaged currents showed more linear than logarithmic profiles. However, Visser (1986), repeated the experiment in the same basin, measured the vertical profiles using micro-propeller and laser Doppler anemometers and found profiles approached more a logarithmic form. In a similar laboratory wave-driven longshore current experiment using laser anemometers, Simons *et al.* (1992) found the vertical velocity profiles tend to show logarithmic behavior. Church *et al.* (1993) used field data from SUPERDUCK experiment (1986) to study the problem. Three electromagnetic current meters mounted on a mobile sled were used in a vertical stack 0.7,

1.0 and 1.5 m above the bed. The results were not conclusive in relation to the logarithmic profile question since only three current meters were used. It was concluded that more current meters located nearer the bed are required to determine the bottom boundary layer shape.

Turbulence induced by breaking waves can modify the vertical profile of longshore currents. The downward vertical momentum mixing produced from the breaking wave-injected turbulence results in a more uniform velocity profile, increasing the shear stress at the bed (Deigaard *et al.*, 1986 and Church and Thornton, 1993).

Wind also modifies the vertical profile of longshore currents. Murray (1975) derived the vertical profiles of mean currents as a function of the wind in shallow water by balancing the surface stress by wind with the bottom stress, with and without the Coriolis force. He compared the theory with observations of current profiles obtained using drogues at various elevations well outside from surf zone. Comparing wind and wave forcing of longshore currents within the surf zone, Whitford and Thornton (1993), showed the wind can be significant, but only at high speed and when the wind has a strong alongshore component.

In the following, mean longshore current profiles obtained over a barred beach are examined with the following objectives:

- a. Test the hypothesis that the turbulent bottom boundary layer of the mean longshore currents is logarithmic.
- b. Determine how breaking-wave induced turbulence generated at the surface modifies the vertical velocity profile.

- c. Investigate how wind modifies the vertical profile of the longshore currents.
- d. Examine the relationship between near bottom vertical velocity profiles and bottom roughness, including the influence of ripples and mega-ripples.



## II. THEORY

The vertical profile of the longshore currents is significantly affected by the physical boundary layers of the bottom and sea surface. The bottom boundary assumes more importance since it determines the general logarithmic profile shape. However, processes in the surface layer can modify the profile in the presence of waves and wind.

### A. BOTTOM BOUNDARY LAYER

Neglecting molecular viscous stresses, the alongshore momentum equation (y-direction) is written

$$\frac{\partial \rho v}{\partial t} + \frac{\partial \rho u v}{\partial x} + \frac{\partial \rho v^2}{\partial y} + \frac{\partial \rho w v}{\partial z} = -\frac{\partial p}{\partial y} \quad (1)$$

Let  $u_i = U_i + u'_i + \tilde{u}_i$  and  $w = w'_i + \tilde{w}_i$ , where the horizontal ( $u_i$ ,  $i=1,2$ ) and vertical  $w$  velocities have been expanded into mean, turbulent and wave-induced components. Assume straight and parallel contours, i.e.,  $\frac{\partial}{\partial y}(\overline{\quad}) = 0$  (overbar indicates time averaging), neglect horizontal turbulent and mean momentum mixing  $\frac{\partial \overline{v'u'}}{\partial x}$ ,  $\frac{\partial UV}{\partial x}$  and neglect  $\frac{\partial \tilde{w}\tilde{v}}{\partial z}$  since its contribution is small above the wave bottom boundary layer. Assuming steady state conditions and after time averaging

$$\frac{\partial \rho \tilde{v}\tilde{u}}{\partial x} = -\frac{\partial \rho \overline{w'v'}}{\partial z} \quad (2)$$

which says the cross-shore change in the wave induced alongshore momentum flux is balanced by vertical changes in alongshore turbulent shear stress. In the shallow water of the surf zone,  $\bar{v}\bar{u}$  can be assumed independent of depth, and its gradient in  $x$  is constant in the  $y$ -direction for straight and parallel contours. Defining

$$\tau_{xy} = -\rho \overline{w'v'} = \rho v_t \frac{\partial v}{\partial z} \quad (3)$$

where  $v_t$  is the turbulent eddy viscosity. Substituting (3) into (2)

$$\frac{\partial \tau_{xy}}{\partial z} = \frac{\partial \rho \bar{v}\bar{u}}{\partial x} = R \quad (4)$$

where  $R$  is constant alongshore. Constant shear stress distributions occur in flows driven by constant hydrostatic pressure gradients, such as in steady open channel flow, which are well described by a logarithmic velocity profile. Therefore it is hypothesized that the vertical velocity profile for longshore currents is logarithmic. A steady, uniform, turbulent boundary layer in the alongshore direction can be described by the logarithmic "law of the wall":

$$v(z) = \frac{v_*}{\kappa} \ln \left( \frac{z + h}{z_o} \right) \quad (5)$$

where  $z$  is positively upward from the surface,  $h$  is the depth of water,  $\kappa$  is the Von Karmann constant (0.4),  $v_*$  is the shear stress velocity and  $z_o$  is the roughness height. The effect of including waves on the bottom stress is to effectively increase the apparent roughness height denoted by replacing  $z_o$  with  $z_a$  (that is analogous to, but larger than  $z_o$ ,

since it includes the additional stress caused by the waves). Following the empirical model by Nielsen (1992) for current profiles in the presence of waves,  $z_a$  can be related to the thickness of wave-dominated layer  $\delta$  by

$$z_a = e^{-1}\delta \quad (6)$$

Since  $\delta$  has no generalized formulation, a particular formula is suggested. For fairly rough conditions ( $0.06 < \frac{r}{A} < 0.5$ ), constant eddy viscosity, and neglecting the angle between wave and current,  $\delta$  can be parameterized as

$$\delta \approx \frac{0.016}{\kappa} \frac{A\omega}{v_*'} r \quad (7)$$

where  $\omega$  is the radian frequency,  $r$  is the hydraulic roughness and  $A$  is the orbital amplitude of the waves just above the bottom wave boundary layer.

The shear stress profile is determined by integrating (4) and assuming the stress at the surface is equal to zero, to give

$$\tau_y(z) = -\tau(-h) \frac{z}{h} \quad (8)$$

where  $h$  is the total depth. Bottom stress is related to  $v_*$  through

$$\overline{\tau_y^b}(z=-h) = \rho v_*'^2 \quad (9)$$

Substituting (5) and (8) into (3) we obtain

$$v_t = -kv_z z(1 + \frac{z}{h}) \quad (10)$$

which says the eddy viscosity is parabolic with depth. However, since it is based on the “law of the wall”, (10) would not be expected to be an adequate formulation near the surface, where the wave and wind effects can be significant.

## B. SURFACE BOUNDARY LAYER

The surface boundary layer is modified by the waves and wind. Wave modifications can be due to three contributions: modification of mean currents by measuring currents in a Eulerian frame with an undulating boundary; contribution to longshore currents of mass transport velocity in the crest-trough region by obliquely incident waves in a Eulerian frame, and modification by the wave breaking.

The most significant modification of the near surface mean current profile is due to the effect of measuring currents in an undulatory wave boundary in a Eulerian frame. In the wave crest/trough region, the averaged measured velocity is decreased because the current meter is out of the water part of the time. For instance, the current meter is out of the water half the time at the MSL, and the time averaged current is only 50% the expected value of the logarithmic profile. To account for this, the surface elevation probability distribution function (*pdf*) is applied to the expected mean current profiles in the absence of waves. The percent of time the current meter is in the water is given by  $1-P(\eta)$ , where  $P(\eta)$  is the cumulative surface elevation *pdf*. In a Eulerian frame of reference, the modified mean current in the crest-trough region is given by



$$V(z) = [1-P(\eta)]V(z) \quad (11)$$

where  $V(z)$  represents the log profile in the absence of waves. For mild wave heights and in deeper water, the surface elevation *pdf* is well described by the Gaussian *pdf*. As will be seen, the measured *pdf*'s in the surf zone are slightly positively skewed from the Gaussian distribution.

The mass transport velocity can contribute to the longshore current in the upper boundary layer when the incident wave angle is relatively large. Assuming irrotational flow and evaluating mass flux (transport),  $M$ , by considering separately two regions in a Eulerian frame of reference (cf. Philips, 1977)

$$M = \rho \left( \int_{-h}^0 u dz + \int_0^{\eta} u dz \right) \quad (12)$$

The first term is zero for irrotational flow. For infinitesimal linear wave theory,  $u$  is not defined between zero and the surface  $\eta$ . A Taylor series expansion about  $z=0$  is used to extend defined values of  $u(0)$  to the surface, giving

$$M = \rho \overline{u(0)\eta} \quad (13)$$

correct to  $O(a/k)^2$ . Applying linear theory

$$M = \frac{E}{\rho C} \quad (14)$$

where  $E$  is the energy and  $C$  the celerity. The mass transport for a single wave is interpreted, to this order in an Eulerian reference frame, as due to a uniform velocity confined to the crest/trough region. The mass transport velocity is defined

$$u = \frac{M}{\rho 2A} \quad (15)$$

where  $A$  is the amplitude.

For random waves, the wave amplitudes are reasonably described by the Rayleigh distribution. The only waves that contribute at any elevation  $z$ , will have an amplitude  $A \geq z$ . Hence, the ensemble average mass transport velocity profile is obtained by applying the wave amplitude *pdf*

$$\langle U(z) \rangle = \int_{z=A}^{\infty} U(A) p(A) dA \quad (16)$$

The Rayleigh distribution is given by

$$p(A) = \frac{8A}{H_{rms}^2} e^{-\left(\frac{2A}{H_{rms}}\right)^2} \quad (17)$$

where  $H_{rms}$  is the *rms* wave height. Substituting (17),  $U(z)$  is given by

$$\langle U(z) \rangle = \frac{\omega}{8 \tanh kh} \frac{H_{rms}}{H_{rms}} \left[ \frac{2z}{H_{rms}} e^{-\left(\frac{2z}{H_{rms}}\right)^2} + \frac{\sqrt{\pi}}{2} \operatorname{erfc}\left(\frac{2z}{H_{rms}}\right) \right] \quad (18)$$

where  $\operatorname{erfc}(x)$  is the complementary error function. The alongshore component is defined by

$$\langle V(z) \rangle = \langle U(z) \rangle \sin \bar{\theta} \quad (19)$$

where  $\bar{\theta}$  is the mean wave incident angle.

The surface boundary layer during wave breaking is typified by an intense production of turbulence that eventually is dissipated in the shear layer at the lower boundary of the surface roller. The remaining energy propagates vertically through the water column. The increase of eddy viscosity due to breaking-induced turbulence produces a more vertical profile of the current for a given shear stress distribution, compared with profiles in the absence of breaking. This results in a stronger velocity gradient near the bed, increasing the bed shear stress.

The influence by wind on the longshore currents can be significant during times of strong alongshore wind. Again integrating (4), but including an alongshore wind stress

$$\int_z^\eta \frac{\partial \tau_{xy}}{\partial z} dz = \tau_y^\eta - \tau_y(z) = R (\eta - z) \quad (20)$$

with  $\tau_y^\eta = \rho_a C_D W W \cos \phi$  (surface) and  $\tau_y^b = \rho C_f \bar{u} v_b$  (bottom), where  $W$  is the wind speed,  $\rho_a$  is the density of air,  $\phi$  the wind angle with the longshore current,  $C_D$  the drag coefficient,  $C_f$  the bed shear stress coefficient and  $v_b$  the longshore current speed at the bottom. Equating the stress at the surface with the alongshore wind stress component we have

$$\tau_y^\eta = \rho v_t \frac{\partial v}{\partial z} \quad (21)$$

Solving for  $v$  exclusively due to the wind

$$v = \frac{\rho_a C_D W^2 \cos \phi}{\rho} \int_{-h}^0 \frac{dz}{v_t} \quad (22)$$

Murray (1975) considered constant  $v_t$

$$v = \frac{\rho_a C_D}{\rho v_t} W^2 \cos \phi \quad h \quad (23)$$

This theory applies when the wind angle to the coast is less than 45 degrees and does not consider the influence of the waves. It is found this treatment overestimates the speed at the bottom, which was verified using field data from DUCK94.

More complex forms can be adopted for eddy viscosity such as the half-parabolic distribution (Roelvink and Reniers, 1994). Here  $v_w$  is defined as

$$v_t = \frac{3}{2} \overline{v_t} \frac{z}{h} \left(2 - \frac{z}{h}\right) \quad (24)$$

with

$$\overline{v_t} = \frac{1}{3} \kappa h \sqrt{\frac{|\tau^\eta|}{\rho}} \quad (25)$$

As will be seen, an exponential distribution of the wind-driven velocity appears to give a reasonable fit to the data

$$v = v_0 e^{\beta z} \quad (26)$$

where  $v_0$  is the velocity at MSL (top current meter) and  $\beta$  a free parameter. The corresponding eddy viscosity is

$$v_t = \frac{\rho_a}{\rho} \frac{C_D W^2 \cos \phi}{v_0} \frac{1}{\beta} e^{\beta(z-h)} \quad (27)$$

This approach is used to interpret the data from DUCK94.



### III. DUCK 94 EXPERIMENT

The measurements described here are part of the comprehensive nearshore DUCK94 experiment conducted during August and October 1994 at the U.S. Army Corps of Engineers Field Research Facility (FRF), Duck, North Carolina. The FRF is located on the Outer Banks, a barrier island formation with no major coastal structures that can obstruct nearshore flows. The beach is a two-bar system with a dynamic inner bar (30-120m offshore) and a secondary bar with lower amplitude (300-400m offshore). The mean foreshore slope of the beach is approximately 0.08 (1:12) and the slope offshore of the bars is approximately 0.006 (1:170) (Lippmann, 1993). The mean tidal range is 1.0 m. Sediments within the surface zone are well sorted with a mean grain size of 0.2 mm. Sediments on the foreshore are poorly sorted with larger mean grain size ( $>0.4$  mm).

A specially designed sled was used as a platform to mount instruments (Fig. 1). The sled is constructed of a 3 x 4 m six-inch aluminum-pipe frame with two 5m, 8 inch pipe runners. This low-profile structure was stabilized by 180 Kg of lead weight plus approximately 450 Kg of sand inside the runners. In addition, four fins (45 cm wide) extended 60 cm into the sand to insure the sled did not move in the surf zone.

The vertical profile of longshore current was measured using a vertical stack of 8 Marsh-McBirney two component electromagnetic current meters with 2.5 cm diameter spherical probes mounted on a 2.5 m mast (Fig. 1). The current meter elevations above the

bed were 23, 42, 68, 101, 147, 179, 224 and 257 cm. The sled was oriented such that the vertical slack of current meters was consistently placed on the "up-current" side of the sled to avoid flow contamination by the sled structure during observations. The current meters were pre- and post- calibrated in a tow tank at the Naval Postgraduate School with an agreement of 1.9 % in gain. An *in situ* determination for the offset is used, which was obtained by reversing the orientation of the current meters on a very slow longshore current day (8 October) by turning the sled around and returning it to the same location (within 1 m) within one hour. The *in situ* determined offsets were within 1 cm/s.

Waves and mean water level were measured using an array of six pressure sensors configured in a 3m square with one in the center and another in the middle of a cross-shore leg.

The data were digitally encoded to 14 bit precision on the sled at 36 samples/second and transmitted to shore via a fibre-optic cable where signals were monitored and recorded. Short cables from the sensors to the data acquisition system on the sled (<7m) resulted in exceptionally low noise electromagnetic current meter and pressure sensor signals. An armored cable, married to the sled chain tether, provided power and controller signals for the instruments via two conductors and returned the digitized signals and video via two fibre-optic lines.

The sled was towed to the farthest offshore location for the first run (approximately 160m from the shoreline) by the Coastal Research Amphibious Buggy (CRAB). A four-



wheel drive forklift pulled the sled shoreward 10 to 30 meters for subsequent runs (each run was nominally one hour). Five to eight runs were made across a transect each day. The data were acquired during daylight to early night.

The morphology of the bottom (bathymetry) was measured at various scales from the CRAB. Large-scale variations of bathymetry were obtained by using an autotracking laser ranging system to measure the CRAB position with a vertical accuracy of less than 3 cm. Contour plots of the bathymetry for the days selected for analysis show the contours in the vicinity of the sled measurements to be quasi straight and parallel (Fig. 2; October 11th is typical). Small-scale vertical bottom variations relative to the CRAB, including ripples and megaripples, were acquired with a 1 MHz sonic altimeter mounted on the CRAB 70 cm from the bed with a vertical accuracy less than 2 cm (Gallenger *et al.*, 1995). Bathymetry for selected days (Fig. 3) shows a pronounced bar progressively moving offshore and significant small-scale morphology in the trough. Areal variations were determined using a 500 KHz side-scan sonar also mounted on the CRAB.

Meteorological information of wind, air temperature, atmospheric pressure and sea surface temperature were recorded simultaneously at the end of the FRF pier and onshore near the FRF laboratory.



#### IV. DATA RESULTS

The data analysis presented is for the October phase of the DUCK94 experiment. The weather during October is climatologically characterized by three distinct phases (Fig.4): weak currents and winds from north (4-9 Oct.), relatively strong currents from north (0.6-1.0 m/s) caused by a storm with predominant winds and waves from north (10-12 Oct.), and variable currents and winds from north/south (13-21 Oct.). The data selected to analyze are 10-12 October, during the strong longshore currents period.

All 22 vertical profiles of longshore currents obtained during the three days are used. The profiles are based on the measurements by seven current meters over the vertical. The current meter the closest to the sea bed was not used because of malfunction. Mean longshore velocities are 1-hour averaged data with the exception of three runs, run 7 on 11 Oct. and runs 6 and 7 on 12 Oct., which are 40-minutes averaged data. In examining the bottom and surface boundary layers, the current meter data are treated separately. For the bottom boundary layer, logarithmic profiles based on a least square method were fit to the data to test the validity of the logarithmic profile hypothesis (Fig.5). The linear correlation coefficients ranged from 0.89 to 0.99 (Table 1). Since the logarithmic velocity profile hypothesis is a bottom boundary layer concept, information from current meters near the surface can be contaminated by the influences of waves and wind and coming in and out of the water and, hence were not included. A criterion is used such that only information from current meters below (MSL-  $H_{rms}$ ), where MSL stands for mean sea level, is considered to

define logarithmic profiles of the bottom boundary layer. This criterion assures the current meters in the analysis came out of the water less than 0.25% of the time based on a Gaussian distribution, which is conservative for the measured skewed distributions. The *rms* wave height is approximated by  $H_{rms} = \sqrt{8\sigma^2}$  where  $\sigma^2$  is the variance calculated from the surface elevation time series. The surface elevation was calculated by Fourier transforming the one-hour pressure record, applying a linear wave theory transfer function to the complex Fourier amplitudes in the frequency domain, and inverse transforming to obtain the surface elevation time series.

In the surface boundary layer, the upper current meters sometimes came in and out of water, which causes noise in the current meter output. To eliminate this noise, when the current meters were within 5 cm beneath the surface or higher as determined from the pressure sensor time series, the current velocities were set to zero.

An example of combining the surface and bottom boundary layers is given in Fig. 6. The bottom is described by a logarithmic profile and the surface boundary layer by the measured surface elevation pdf (equation 11).

The velocity profiles at successive offshore positions (runs) that the sled occupied during a transect are shown in Fig. 7. The data agree well with the logarithmic profile. The largest discrepancies occur over the bar, where wave breaking is most intense (x-distance between 220 and 240 m). The largest deviation occurs for the fourth run of 11 Oct, which generated an outlier in the parameter estimates. The average correlation for all *u* profiles between log elevation and longshore velocity is 0.98; this value is decreased by the observations in the breaking zone (over the bar).

The value of  $z_a$  is calculated from the intersection of the linear regression least squares fit to the data in semi-log form, and the shear stress velocity  $v_*$  is estimated from the slope. In addition, the bed shear stress coefficient,  $C_f$ , can be calculated from the data. Assuming a quadratic bed shear stress relationship

$$\tau_y^b = \rho C_f \overline{(u^2 + v^2)^{\frac{1}{2}} v} \quad (28)$$

and combining with (8), gives

$$C_f = \frac{v_*^2}{(u^2 + v^2)^{1/2} v} \quad (29)$$

A mean eddy viscosity for each run is defined by integrating (10)

$$\bar{v}_t = kv_* \frac{h}{6} \quad (30)$$

Values of  $z_a$ ,  $v_*$ ,  $C_f$  and  $\bar{v}_t$  are given in table 1.

An attempt is made to find relationships between the calculated parameters  $C_f$ ,  $z_a$  and  $\bar{v}_t$  with physical measurements such as  $\frac{u_m}{V}$  (ratio of near-bottom wave velocity magnitude to mean current measured at lowest current meter),  $\gamma = \frac{H_{rms}}{h}$  (% of wave breaking) and the *rms* bottom roughness,  $r$ , measured by the CRAB's altimeter. An example of the variation of *rms* bottom roughness calculated over 20 m detrended sections, in one meter steps across the surf zone is shown in Fig. 8. Bottom roughness is smoothest offshore and over the bar with increased roughness within the trough.

The data are qualitatively sorted by location over the bar, in the trough and on the foreshore. This method allows a better identification of the possible correlations among variables.

In general,  $C_f$  and  $z_a$  values increased an order of magnitude across the surf zone.  $C_f$  values were lowest over the bar and tended to vary over a small range for all values of  $\frac{u_m}{V}$  (Fig. 9).  $C_f$  tended to increase with increasing  $\frac{u_m}{V}$  over the trough area.  $\frac{z_a}{h}$  tended to behave in a similar manner to  $C_f$  (Fig. 10).  $C_f$  does increase with bottom roughness (Fig. 11).  $C_f$  is also plotted against  $\frac{r}{A}$  (Fig. 12) where  $A$  is the wave orbital excursion amplitude, which, for linear shallow water wave theory is given by

$$A = \frac{H_{rms}}{T} 2\pi \sqrt{\frac{h}{g}} \quad (31)$$

where  $g$  is the gravity constant.  $\frac{z_a}{h}$  also tends to increase with  $\frac{r}{A}$  (Fig. 13).

Analyzing the parameters over the cross-shore distance,  $C_f$  increases slightly toward the beach but this smooth trend is interrupted with a sharp peak in the wave breaking area. After this  $C_f$  returns to the previous behavior (Fig. 14).  $\bar{v}_t$  shows minimum values over the bar, a peak in the trough region and decreasing values on the foreshore, reflecting that it is calculated as the product of  $v_* h$  (Fig. 15). Plots of  $C_f$  or  $\frac{z_a}{h}$  versus  $\gamma = \frac{H_{rms}}{h}$  show poor correlation (Figs. 16 and 17).

The wind contribution to the longshore currents was evaluated by plotting an exponential approximation (26), used to model the wind-driven portion of the profiles, and compared with the residual of the measured surface elevation pdf (Fig. 18). The exponential

approximation shows, in general, good agreement with the residual. The wind data is summarized in Table 2.





## V. DISCUSSION

There has been a lack of field data to describe the mean vertical velocity profile of longshore currents. Three days of DUCK94 experiment when strong longshore currents occurred were examined. Mean currents obtained using seven current meters spaced from 41 to 257 cm above the sea bottom, were well described by a logarithmic profile. The validity of the logarithmic approach is reflected in a high correlation mean value of 0.98 for all 22 profiles, between the log elevation of the current meters and the measured velocities. The largest deviations occurred over the bar and the foreshore, related to the increased turbulence caused by wave breaking.

A sensitivity test was performed to determine if the correlation coefficient changed with the number of current meters used to define the profile. Using either all the current meters available under the criteria established in chapter 4, or only the lowest three or four, the correlations are similar with maximum changes of only 0.02. This demonstrates the validity of the logarithmic approach over most of the water column. In the same way, the values of  $C_f$  do not significantly change when calculated with only the lowest current meters.

In the breaking zone the values of the bed shear stress coefficient (or bottom friction coefficient),  $C_f$ , are in the order of  $10^{-2}$  while the rest of the transect shows  $C_f$  values in the order of  $10^{-3}$  (consistent with previous experiences in the same beach).

There is some uncertainty of the exact distance of the current meters from the bed, because the sled runners sunk into the sand an unknown amount depending on bearing capacity of the bed (theory and divers suggest 3-8 cm) and the undulating bottom, particularly over mega-ripples. To test the sensitivity of  $C_f$  due to the uncertainty in depth, the elevation of the current meters was shifted  $\pm 20$  cm in steps of 1 cm and  $C_f$  recalculated. An average value of  $\Delta C_f = 0.001/10\text{cm}$  was calculated (5 to 30 % of calculated  $C_f$ ). The changes of  $C_f$  are less significant for increased depth (-20 cm) than for decreased depth (+20cm).

$C_f$  and  $\frac{z_a}{h}$  show surprisingly poor correlation with the wave/current parameter  $\frac{u_m}{V}$ , since it was expected an increasing of  $C_f$  and  $\frac{z_a}{h}$  with increasing values of  $\frac{u_m}{V}$  (increasing of the wave influence over the vertical profile). Equation (6) suggests a relationship between  $z_a$  and wave parameters. For shallow water waves (6) can be rewritten

$$\frac{z_a}{h} \approx e^{-1} \frac{0.016}{\kappa} \sqrt{g} \frac{H_{rms}}{h^{3/2}} \frac{r}{v_*} \quad (32)$$

Equation (32) combines wave, current and roughness variables.  $\frac{z_a}{h}$  is plotted against equation (32) expression in Fig.19. However, including wave and current variables with roughness makes the correlation with  $z_a$  worse.

The strongest correlation was found between  $C_f$  and the bottom roughness, with  $C_f$  increasing with the bottom roughness. Theoretically this is expected as larger roughness implies larger bottom stress due to form drag, and consequently larger  $C_f$  values.  $z_a$  also increased with the bottom roughness ( $\frac{r}{A}$ ), but not as strongly as  $C_f$ . The  $C_f$  values varied

by an order of magnitude across the surf zone. This implies that the bottom roughness has an important role in the characterization of the bottom boundary layer by affecting the value of  $C_f$ . Roughness values increase toward the beach and are larger in the trough. The increased roughness of the bottom in the trough is associated with mega-ripples observed by side-scan sonar (Swayne, 1995).

The behavior of  $\bar{v}_t$  along the cross-shore line is basically a function of the velocities and the depth. Low values over the bar and foreshore (smaller  $h$ ) and high values over the trough (larger velocities) are explained by (30).

Wind contribution to the longshore current was examined. Using a simplified approach, reasonable agreement was found between an exponential approximation and the residual of velocity/surface elevation pdf correction. Nevertheless it is difficult to predict if the residual is due only to the wind or if other factors, such as mass transport velocity or wave breaking also contribute to this residual. The free parameter  $\beta$  in equation (26) varied between 3 and 4 giving reasonable predictions for the cases studied. Since the approximation was tested over only 12 profiles, future work is needed to refine the value of  $\beta$ .



## VI. CONCLUSIONS

The vertical structure of mean longshore currents on a barred beach is well described by a logarithmic profile for the three strong longshore current days examined. This hypothesis works better in the trough where turbulent bottom boundary layer processes are more dominant than over the bar, where breaking-wave induced turbulence generated at the surface modifies the profile.

A relationship between near bottom vertical velocity profiles and bottom roughness was found. While the relatively small amount of data used (three days) are not enough to establish a definitive conclusion from the available data, it can be concluded that the bed shear stress coefficient  $C_f$  is directly proportional relationship to the bottom roughness and therefore is an important parameter to characterize the bottom boundary layer. Surprisingly, only poor correlation of  $C_f$  and  $z_a$  was found with wave parameters.

The influence of the wind is parameterized by an exponential approximation that works well in 50% of the analyzed profiles. This parameterization assumes that the residual between the velocity corrected using the surface elevation pdf and the measured data is only due to the wind and does not consider the alongshore component of mass transport velocity that is assumed small.

These results should be treated carefully since there were obtained from a small number of days over a barred beach with strong longshore currents and cannot be generalized without further studies.



## APPENDIX A. FIGURES





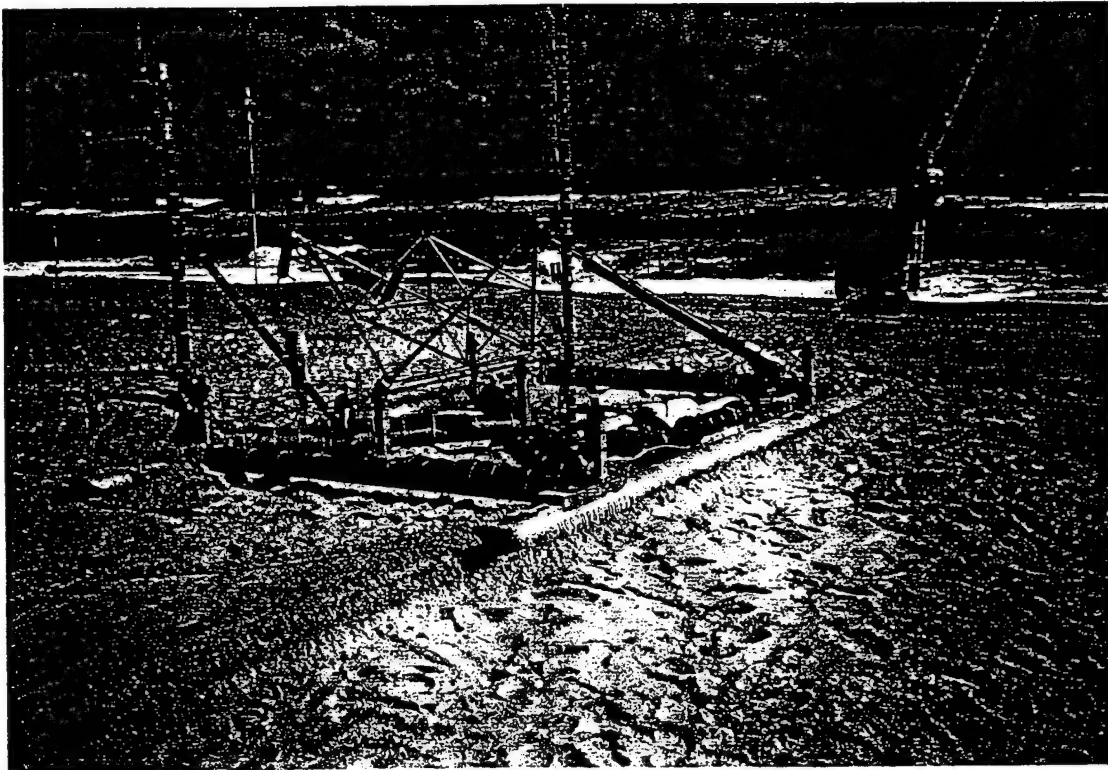


Figure 1. SLED on the beach during DUCK94 experiment.

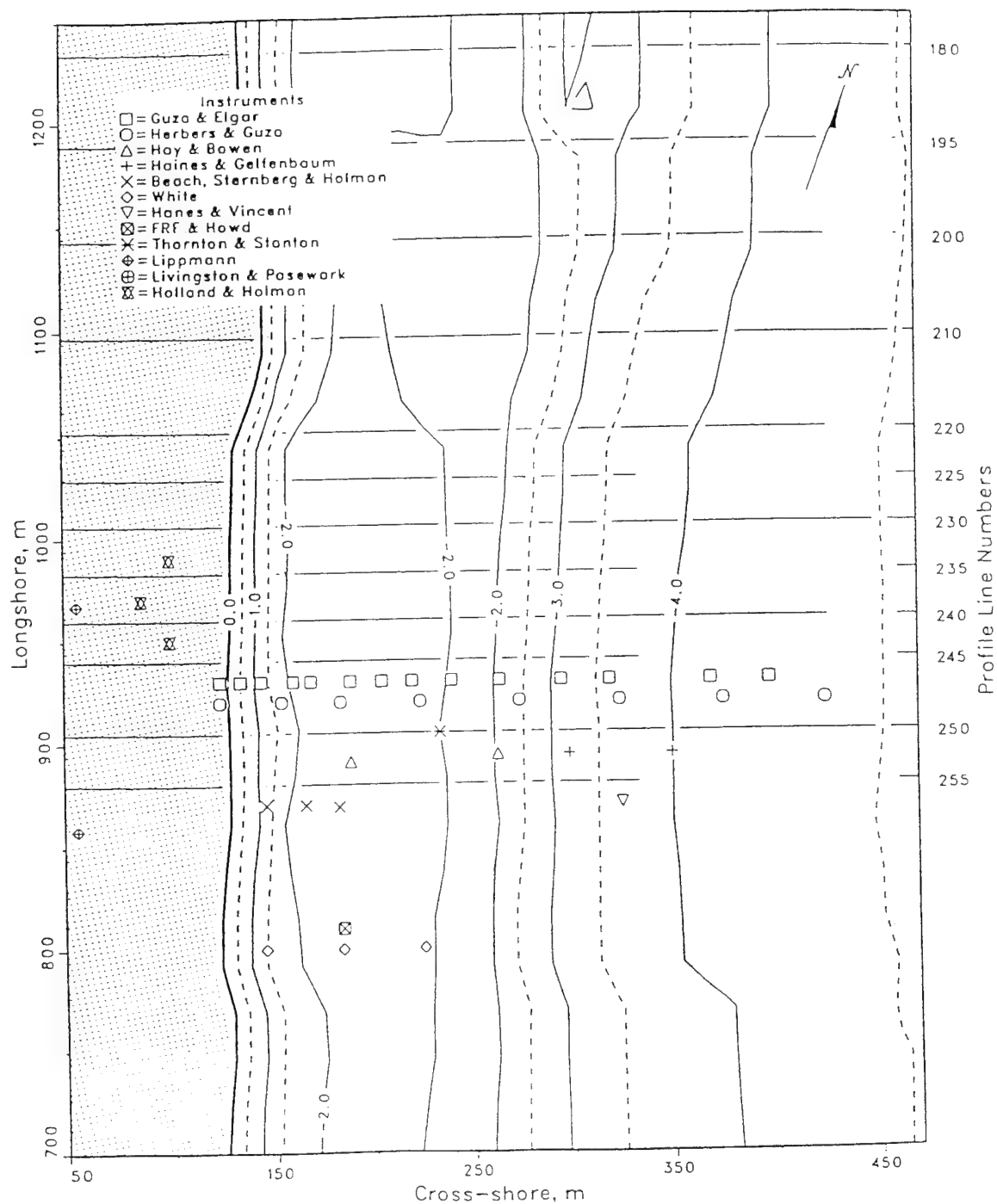


Figure 2. Bathymetry and equipment positioning during DUCK94 experiment (11 Oct.). Sled transect line was 940 m alongshore.

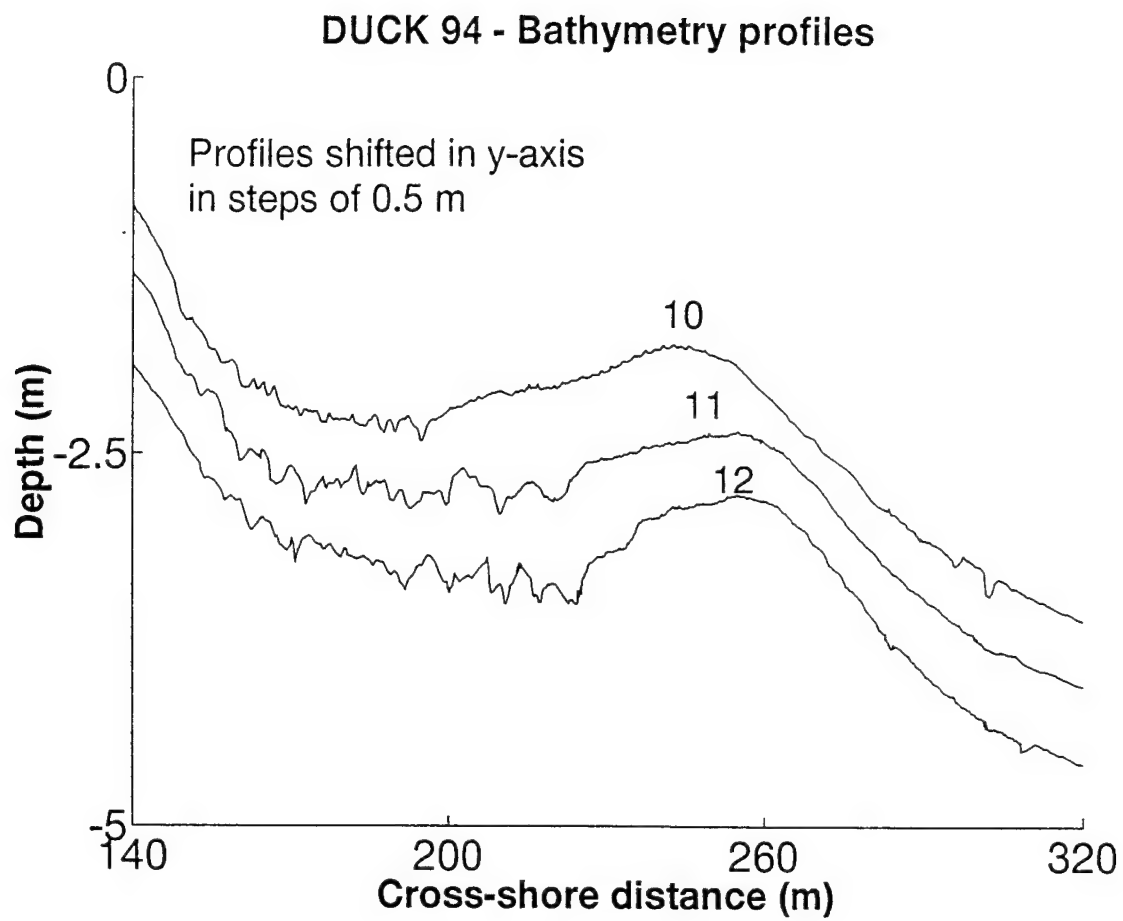


Figure 3. Bathymetry profiles for the three days considered (10, 11 and 12 Oct.).

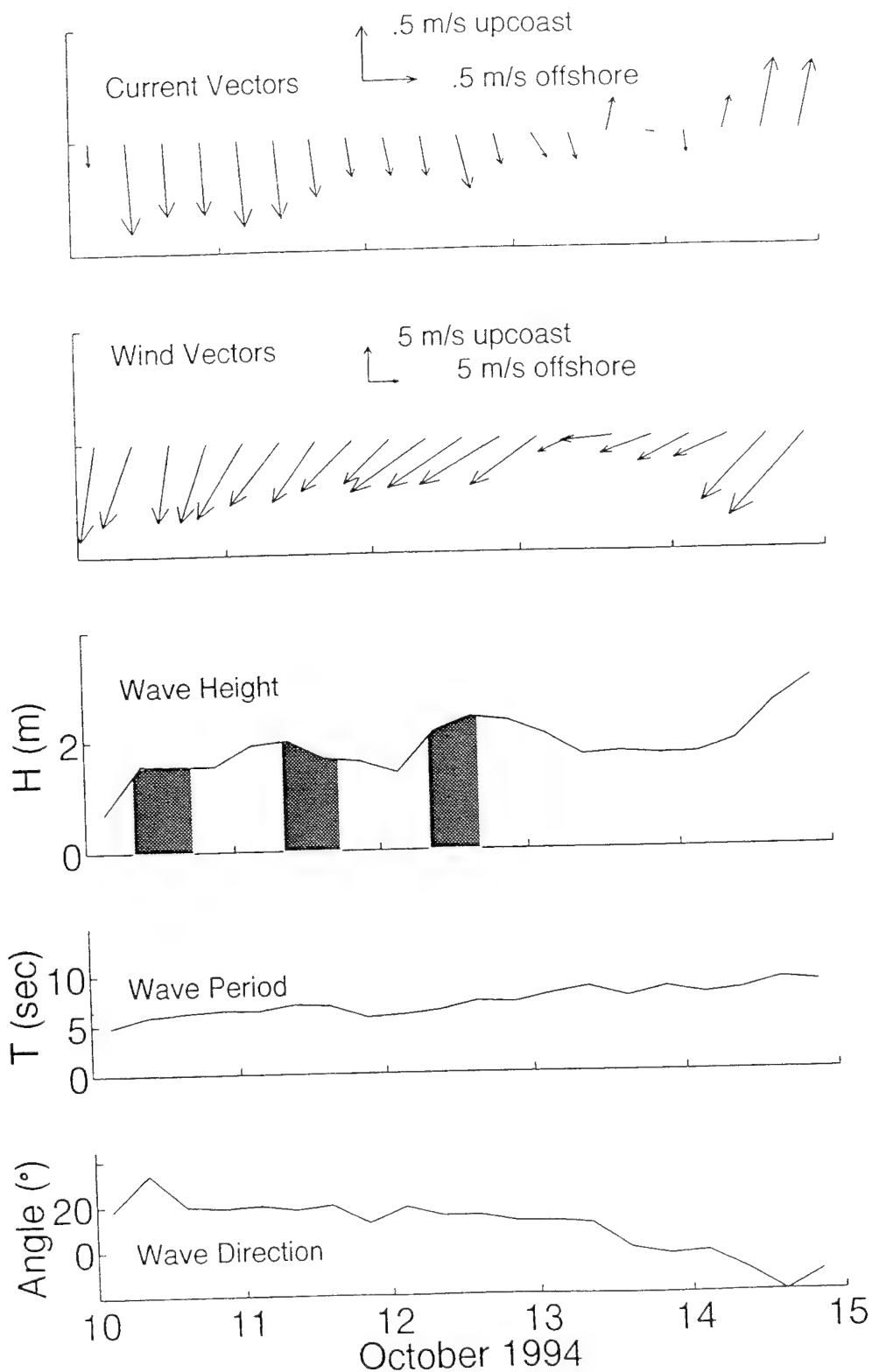


Figure 4. Climatology for the three days considered (10, 11 and 12 Oct.). Currents were measured in the middle of the trough.  $H$  is the significant wave height and  $T$  is the period of peak frequency.

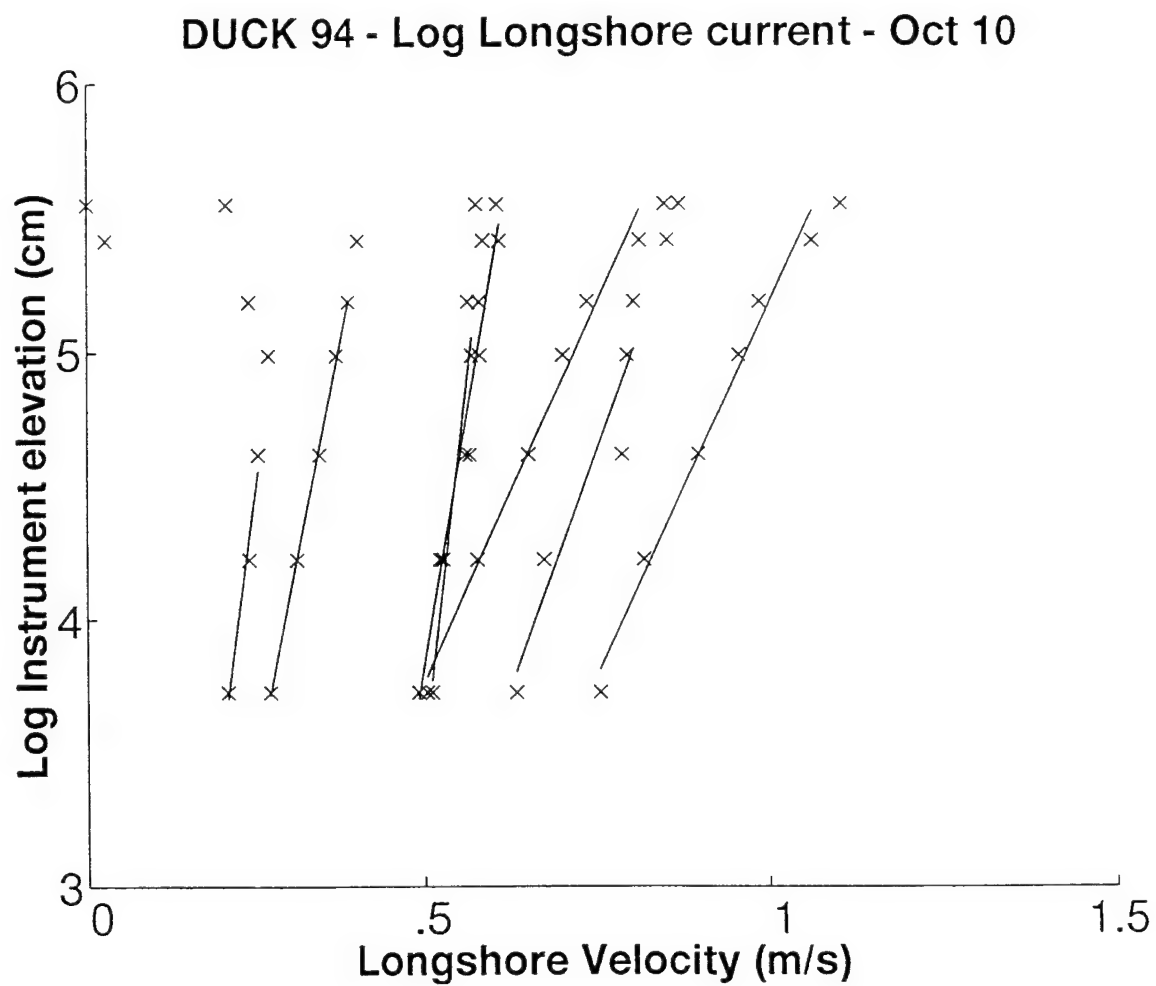


Figure 5. (a) Least-squares fit to the data for 10 Oct.

DUCK 94 - Log Longshore current - Oct 11

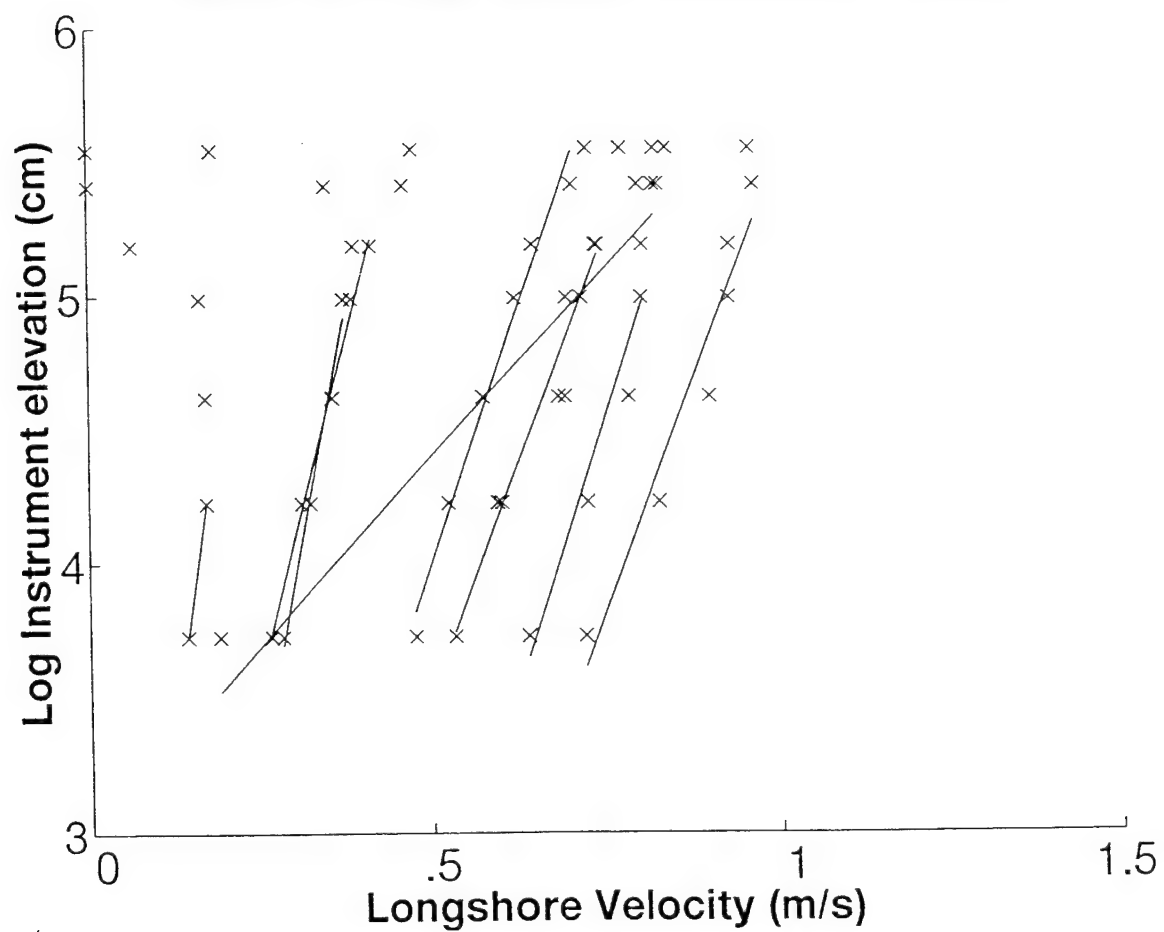


Figure 5. (b) Least-squares fit to the data for 11 Oct.

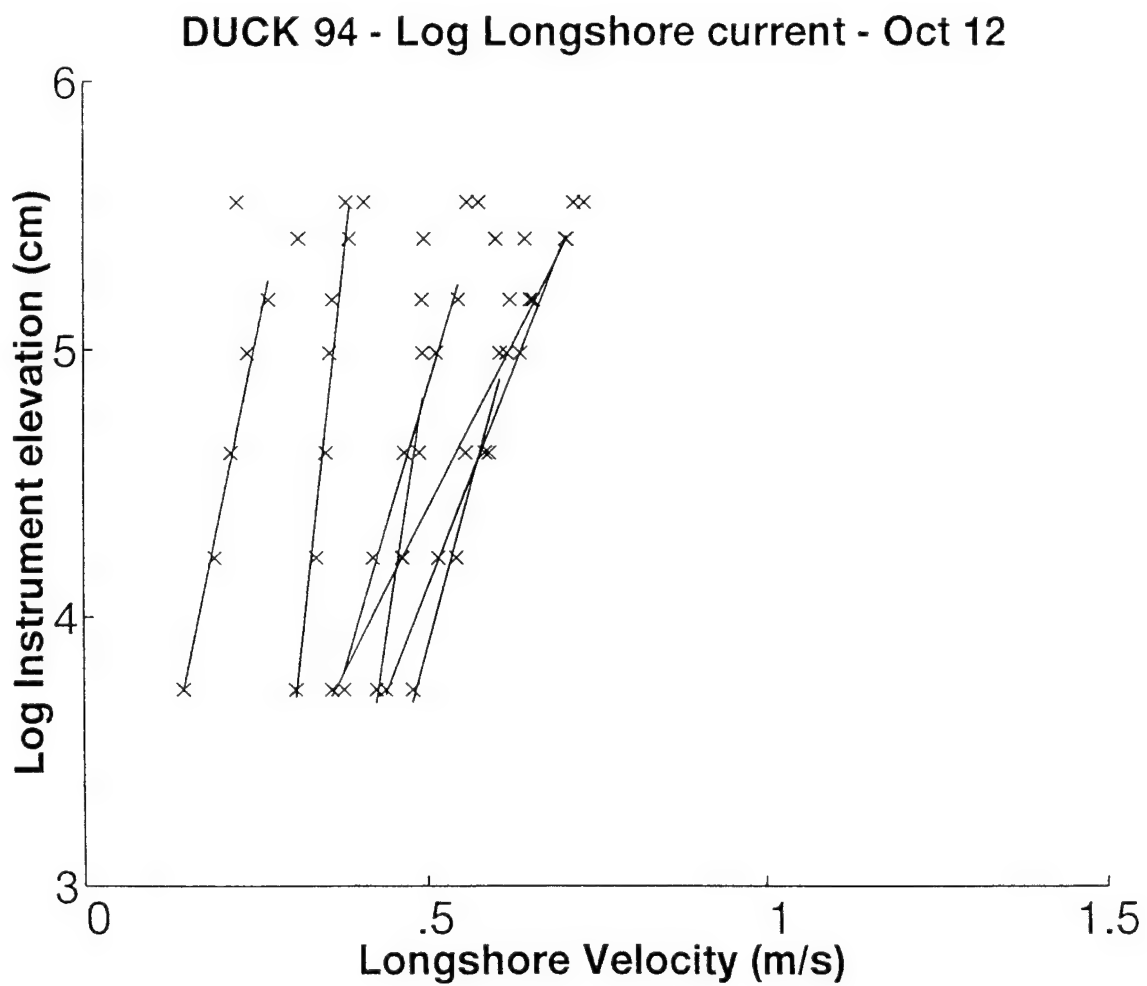


Figure 5. (c) Least-squares fit to the data for 12 Oct.

DUCK 94 - Longshore current - Oct 11 time 15:44 - xposition = 157.3

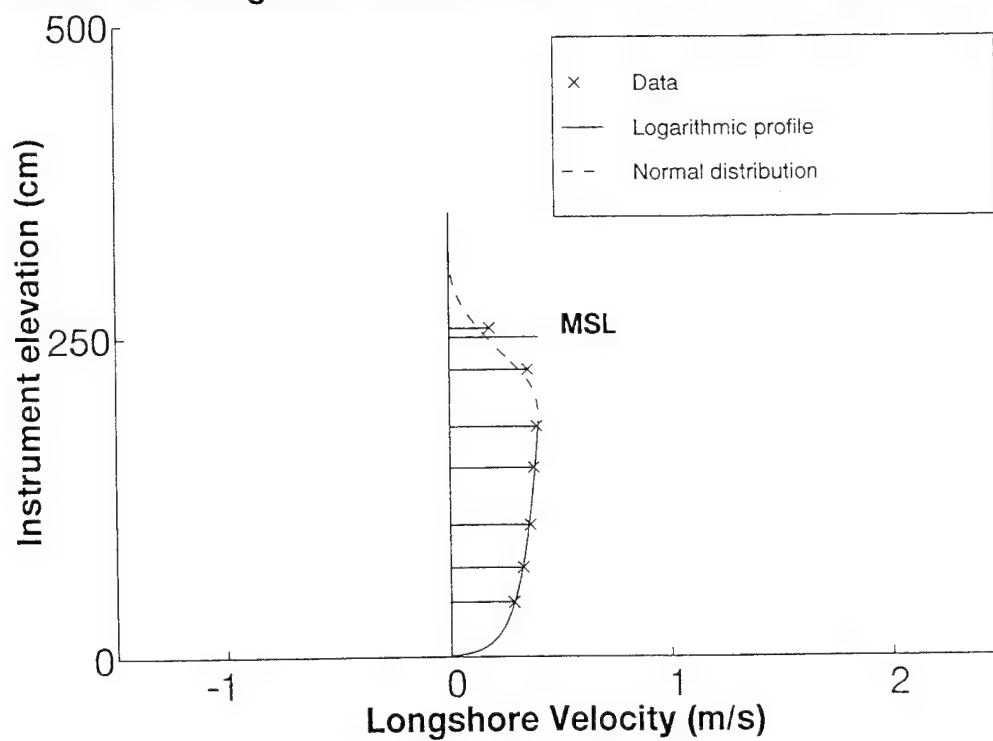


Figure 6. Example of vertical profile (the upper two current meters sometimes were out of the water).



# DUCK 94 - Longshore current - Oct 10

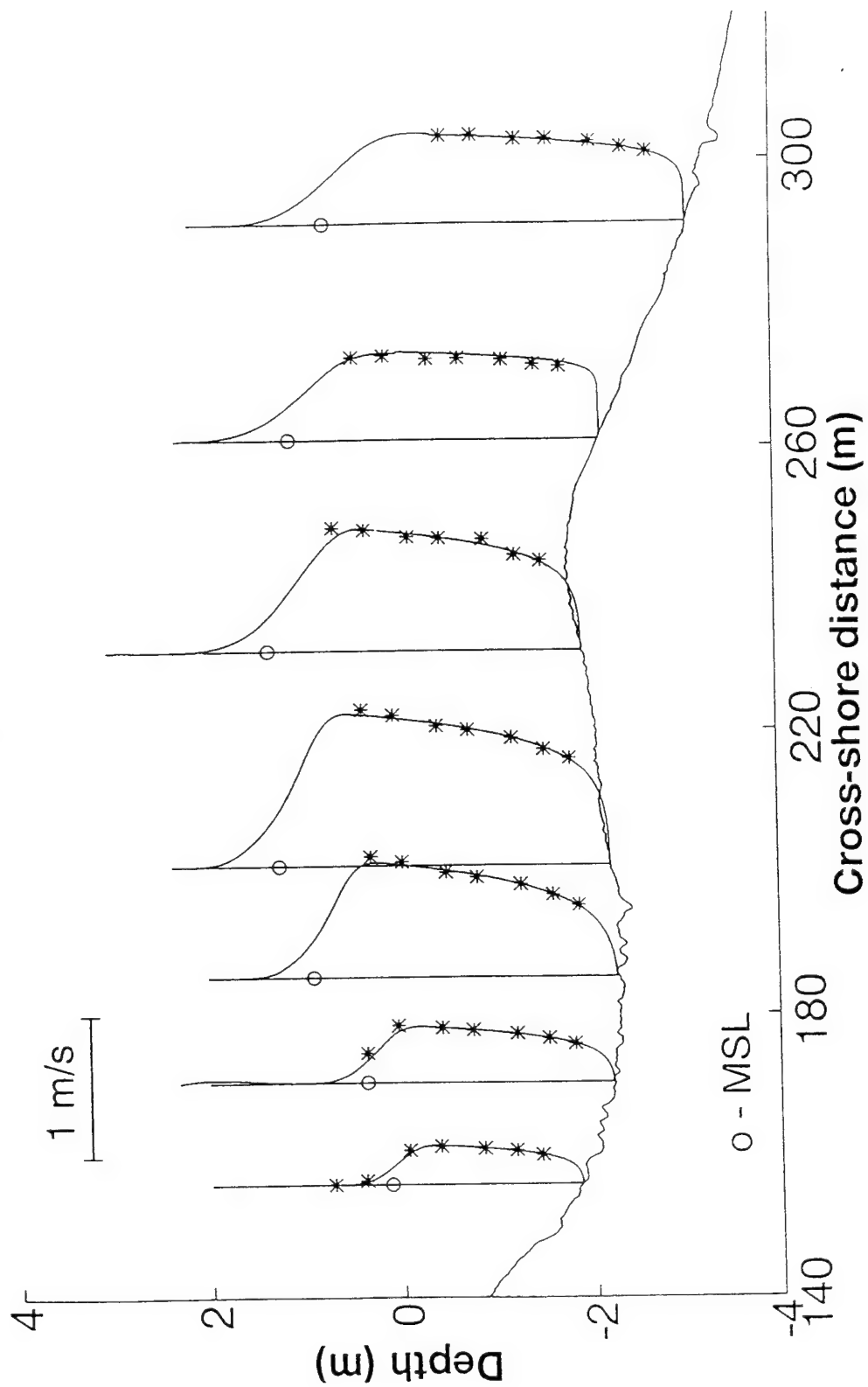


Figure 7. (a) Vertical profiles of mean longshore currents for 10 Oct.

# DUCK 94 - Longshore current - Oct 11

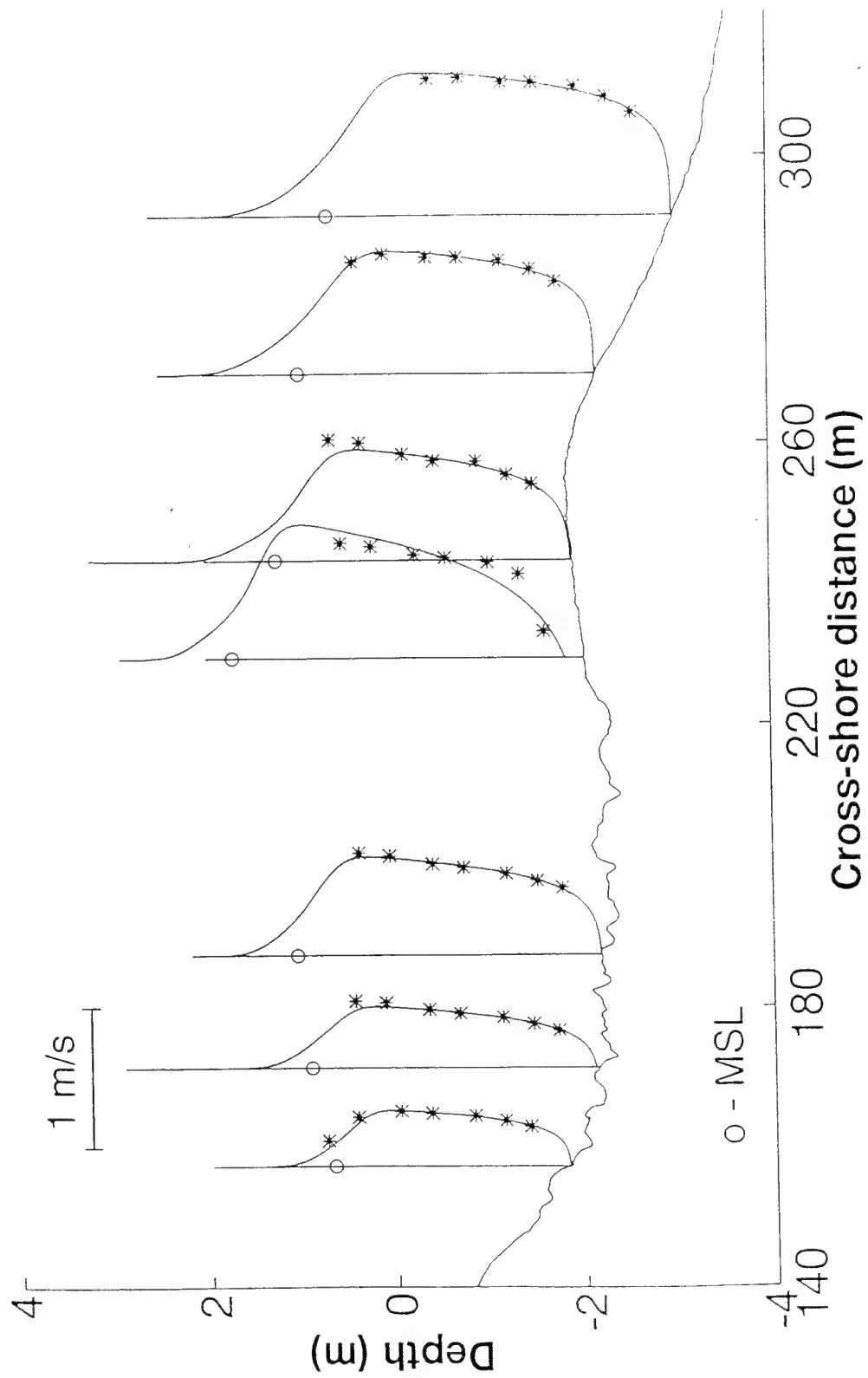


Figure 7. (b) Vertical profiles of mean longshore currents for 11 Oct.

# DUCK 94 - Longshore current - Oct 12

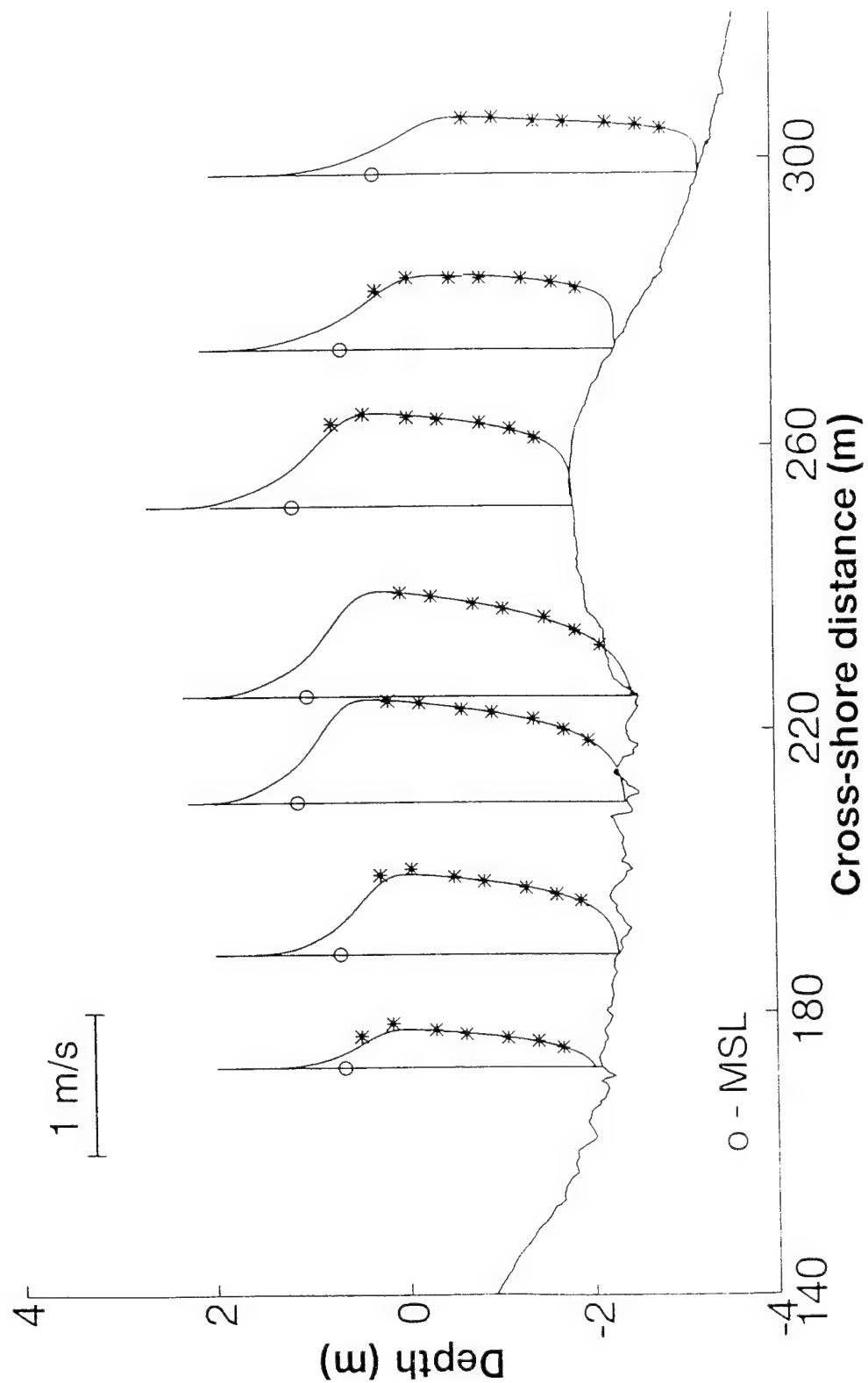


Figure 7. (c) Vertical profiles of mean longshore currents for 12 Oct.

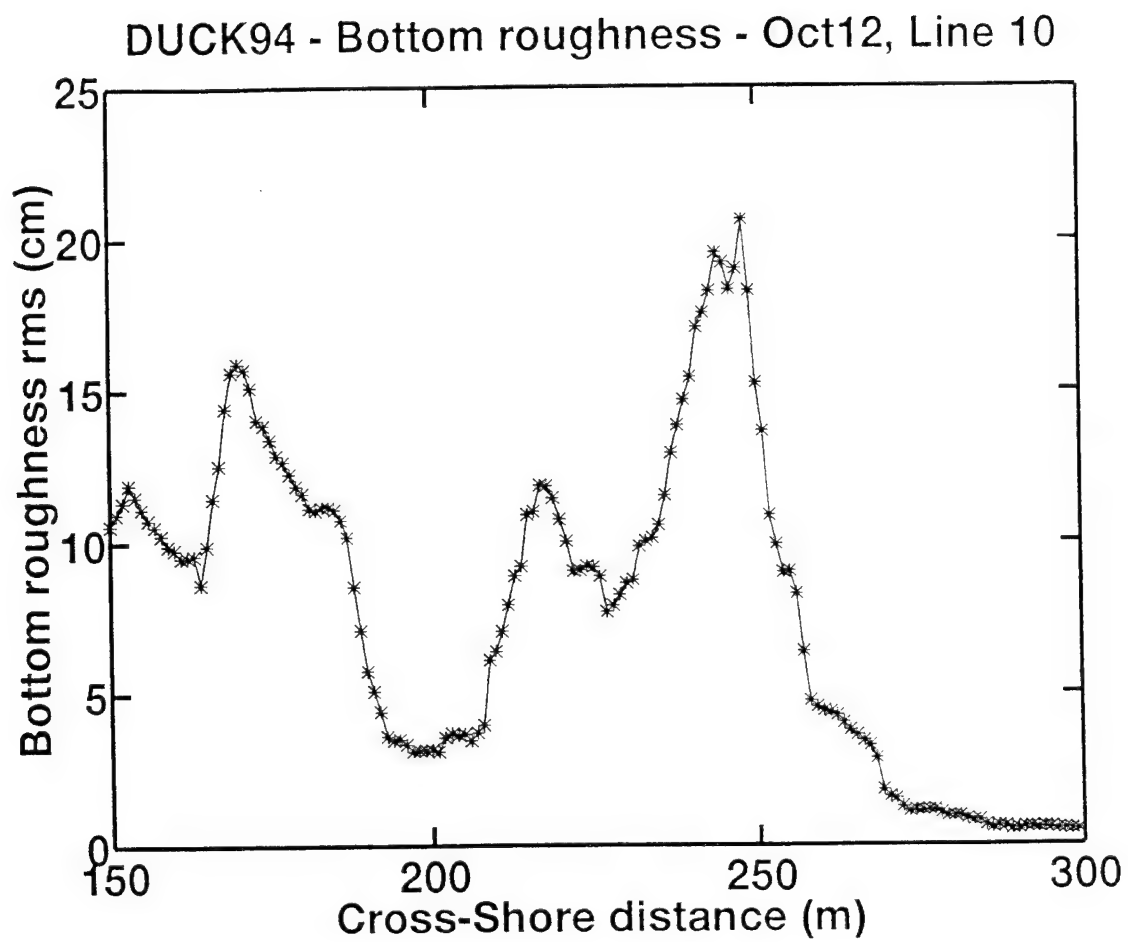


Figure 8. Variation of the *Rms* Bottom Roughness with the Cross-Shore Distance

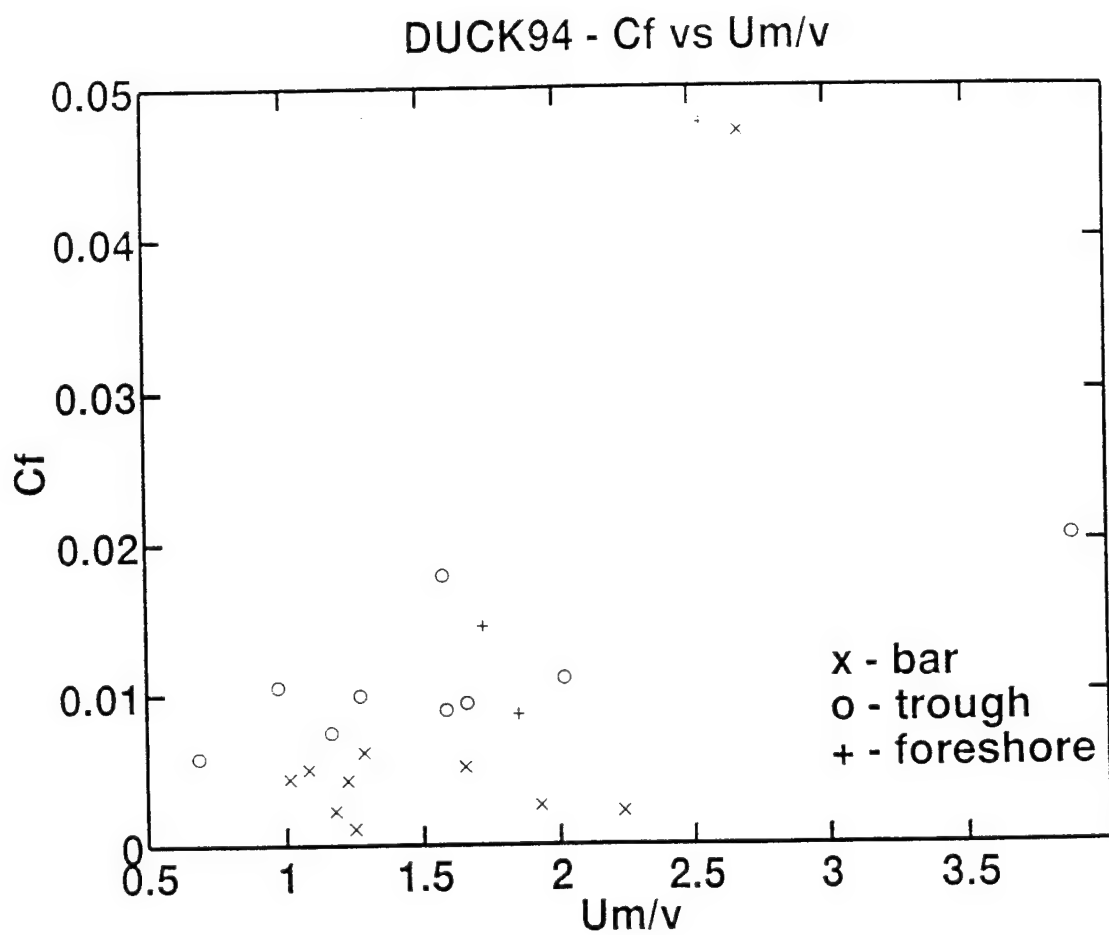


Figure 9. Relationship Between  $C_f$  and  $U_m / V$ .

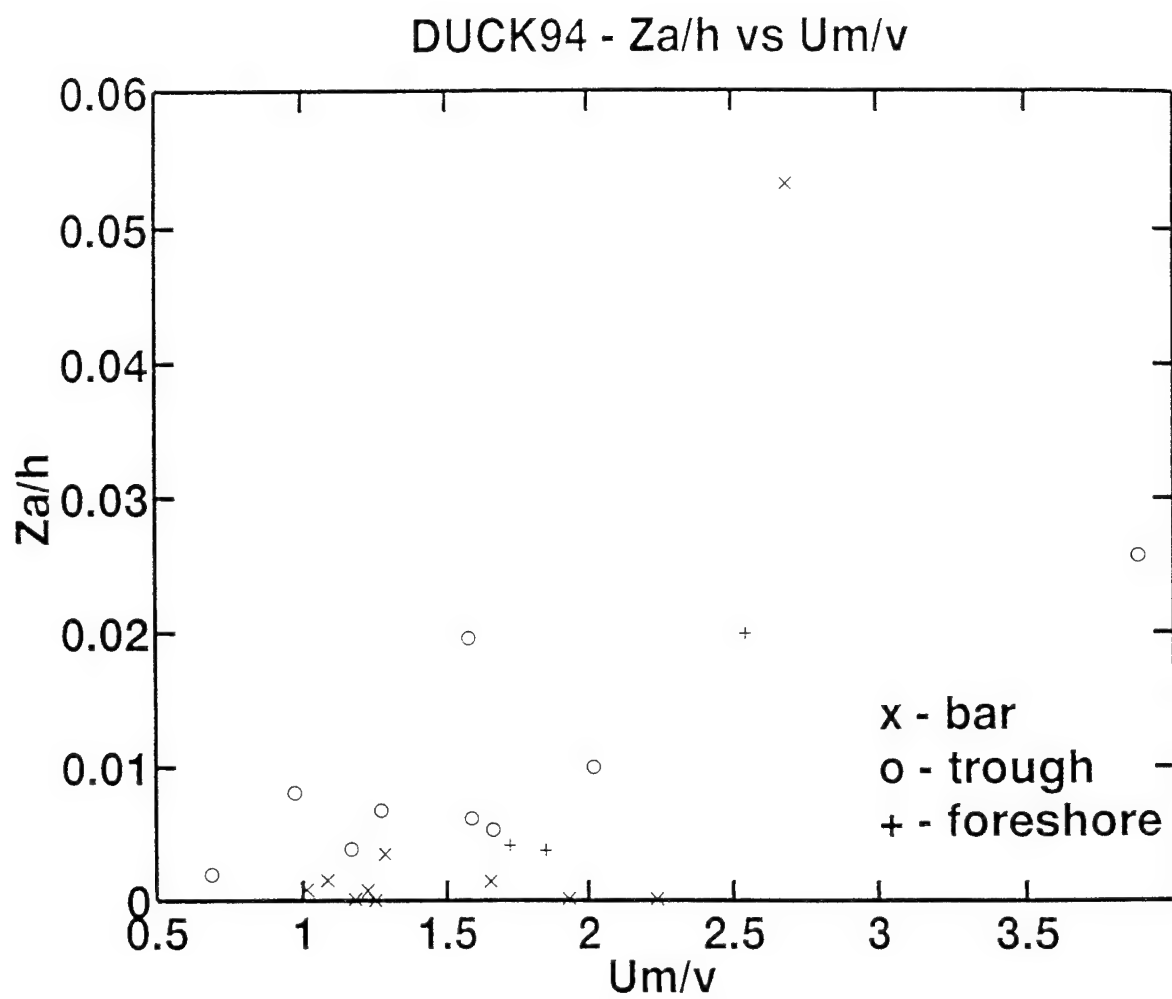


Figure 10. Relationship Between  $\frac{z_a}{h}$  and  $U_m / V$ .

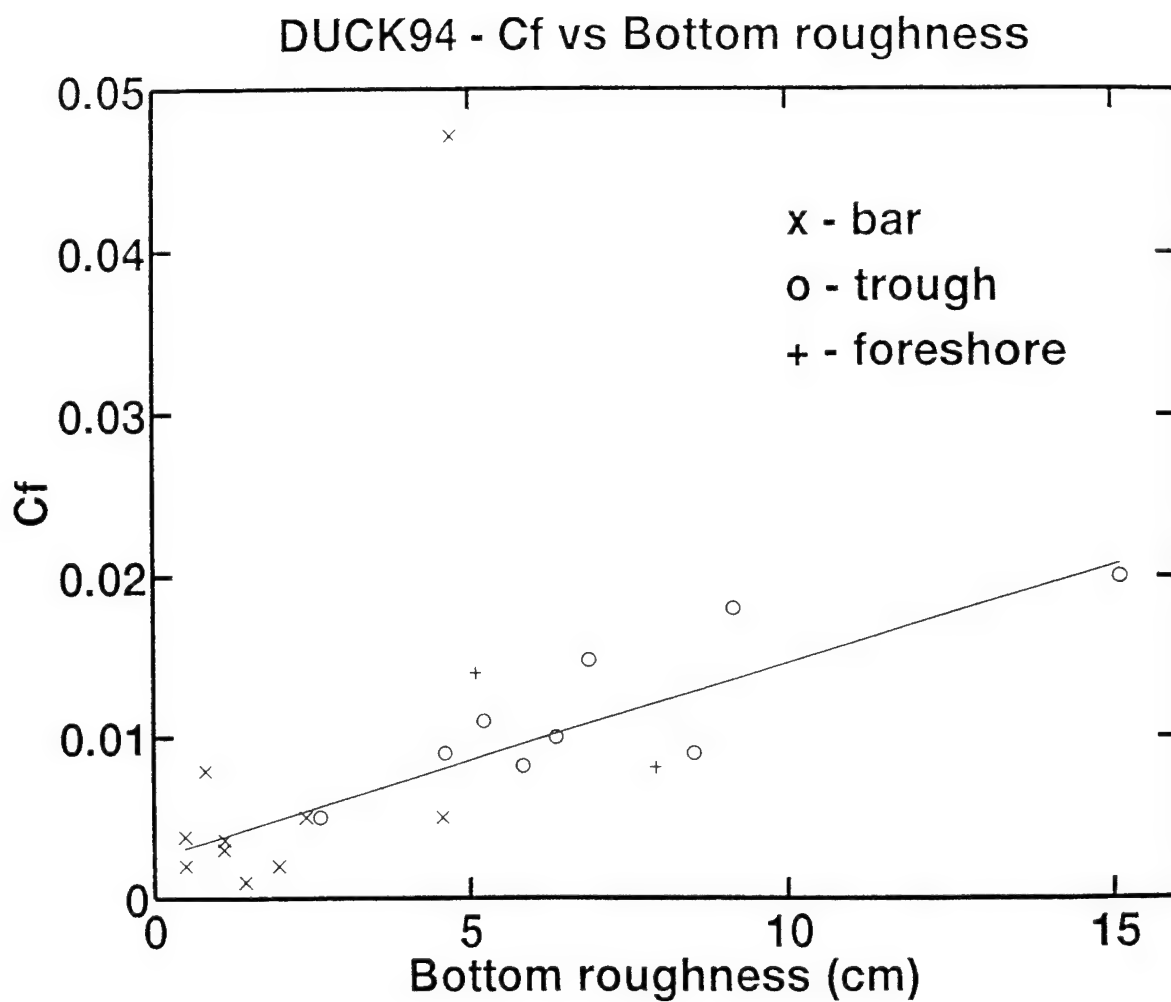


Figure 11. Bed Shear Stress versus Bottom Roughness. The Line Represents a Linear Regression Based on All Points but the Outlier.

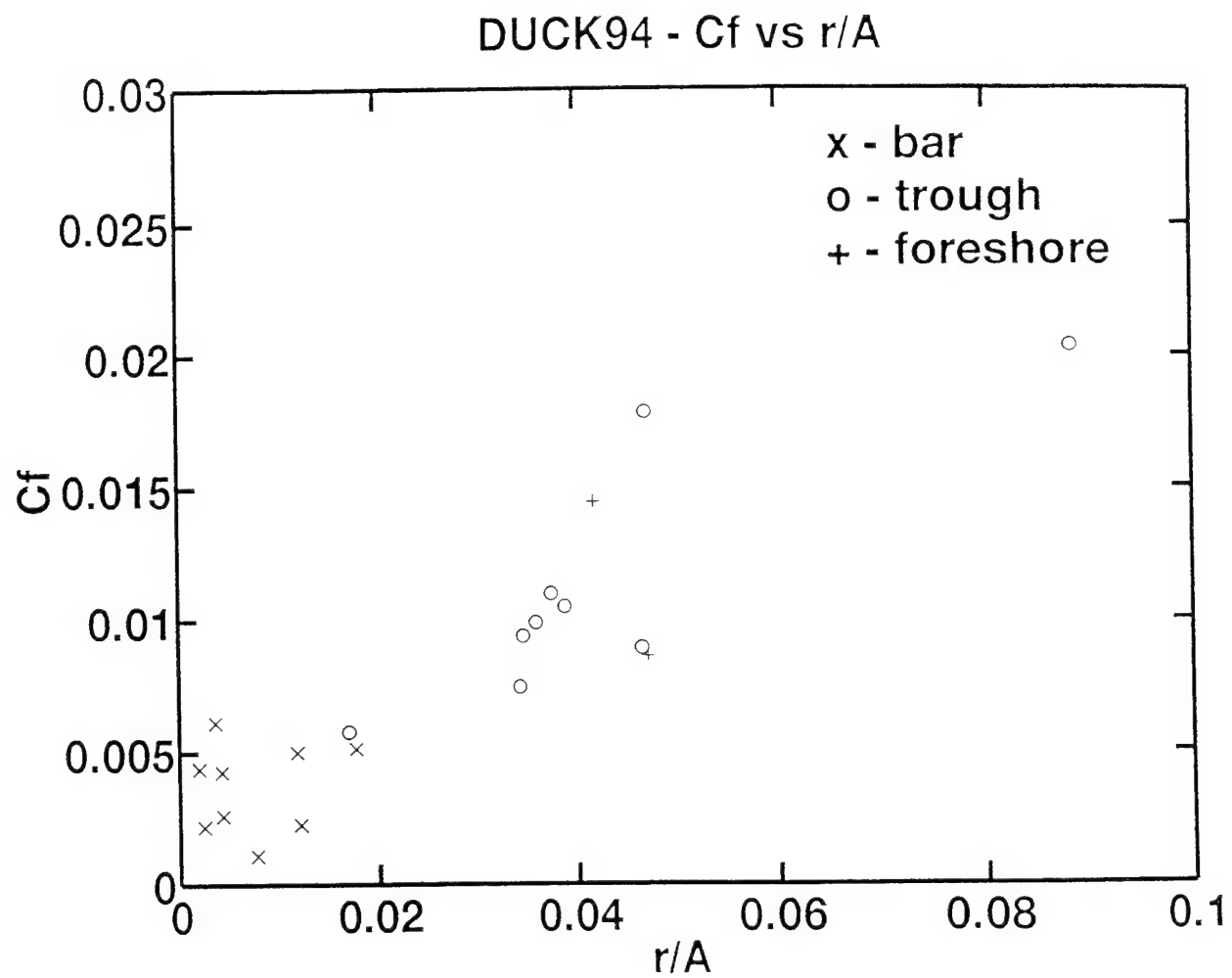


Figure 12.  $C_f$  versus  $\frac{r}{A}$



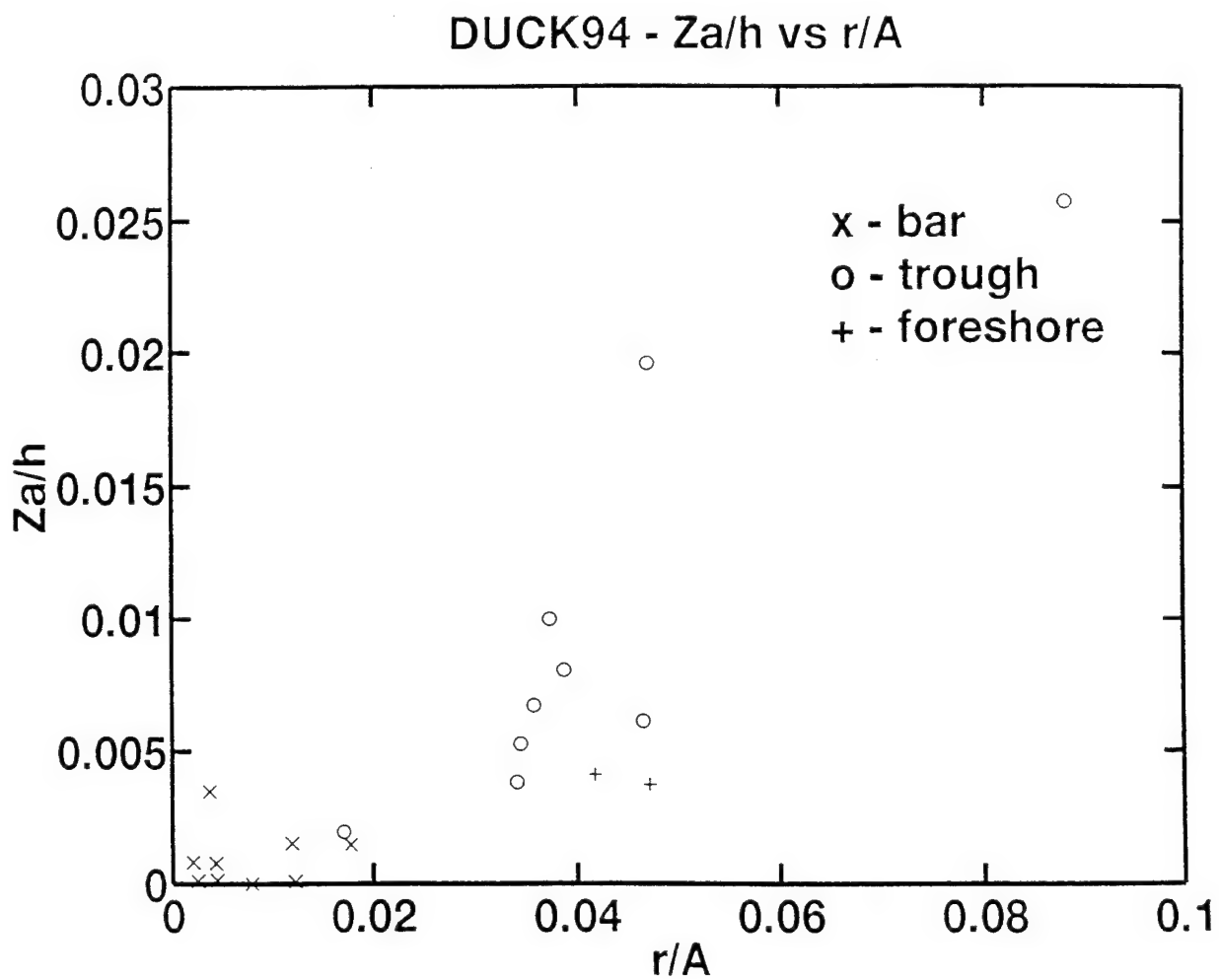


Figure 13.  $\frac{z_a}{h}$  versus  $\frac{r}{A}$  (Outlier not Included).

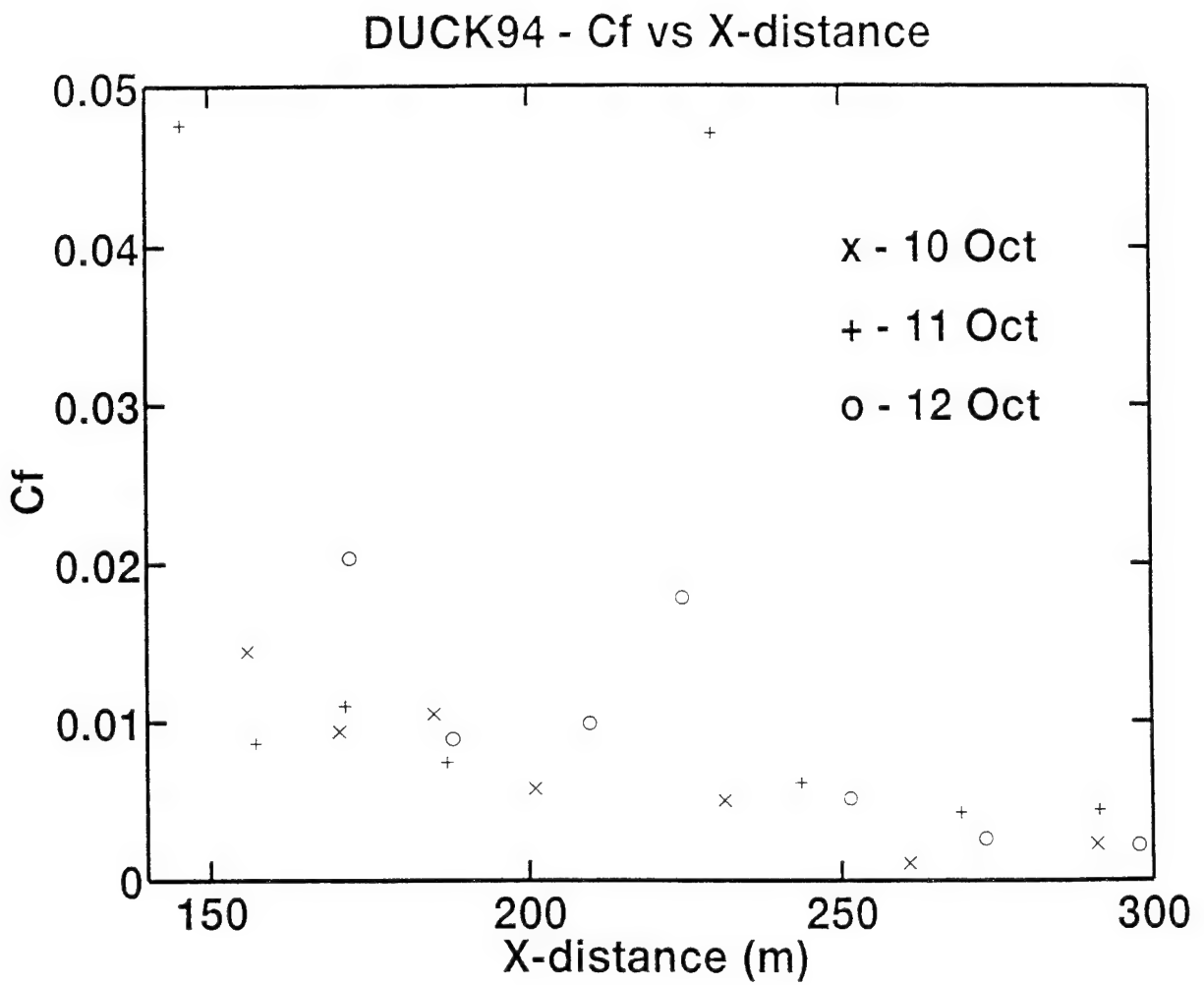


Figure 14.  $C_f$  versus Cross-Shore Distance.

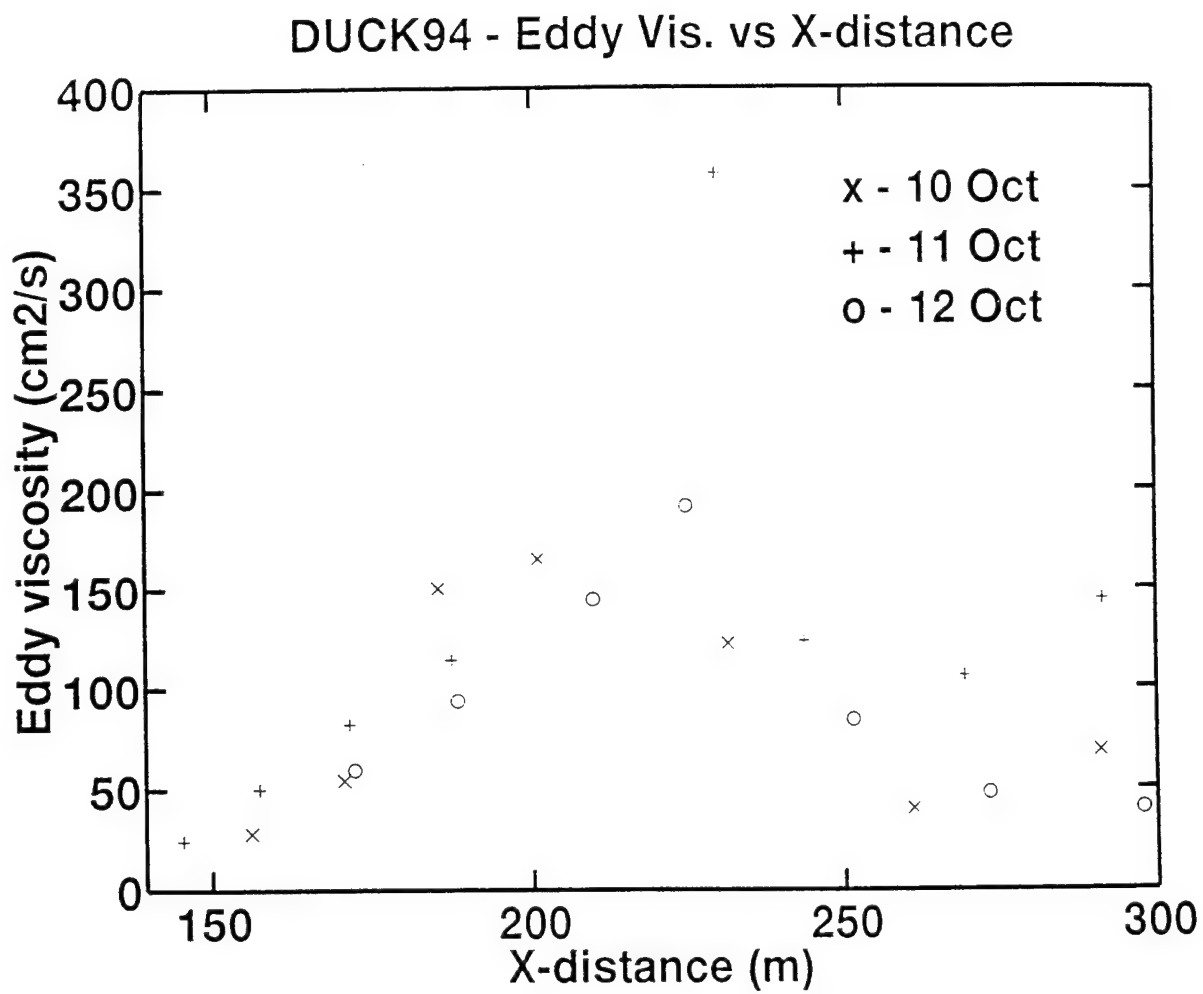


Figure 15  $v_t$  versus Cross-Shore Distance.

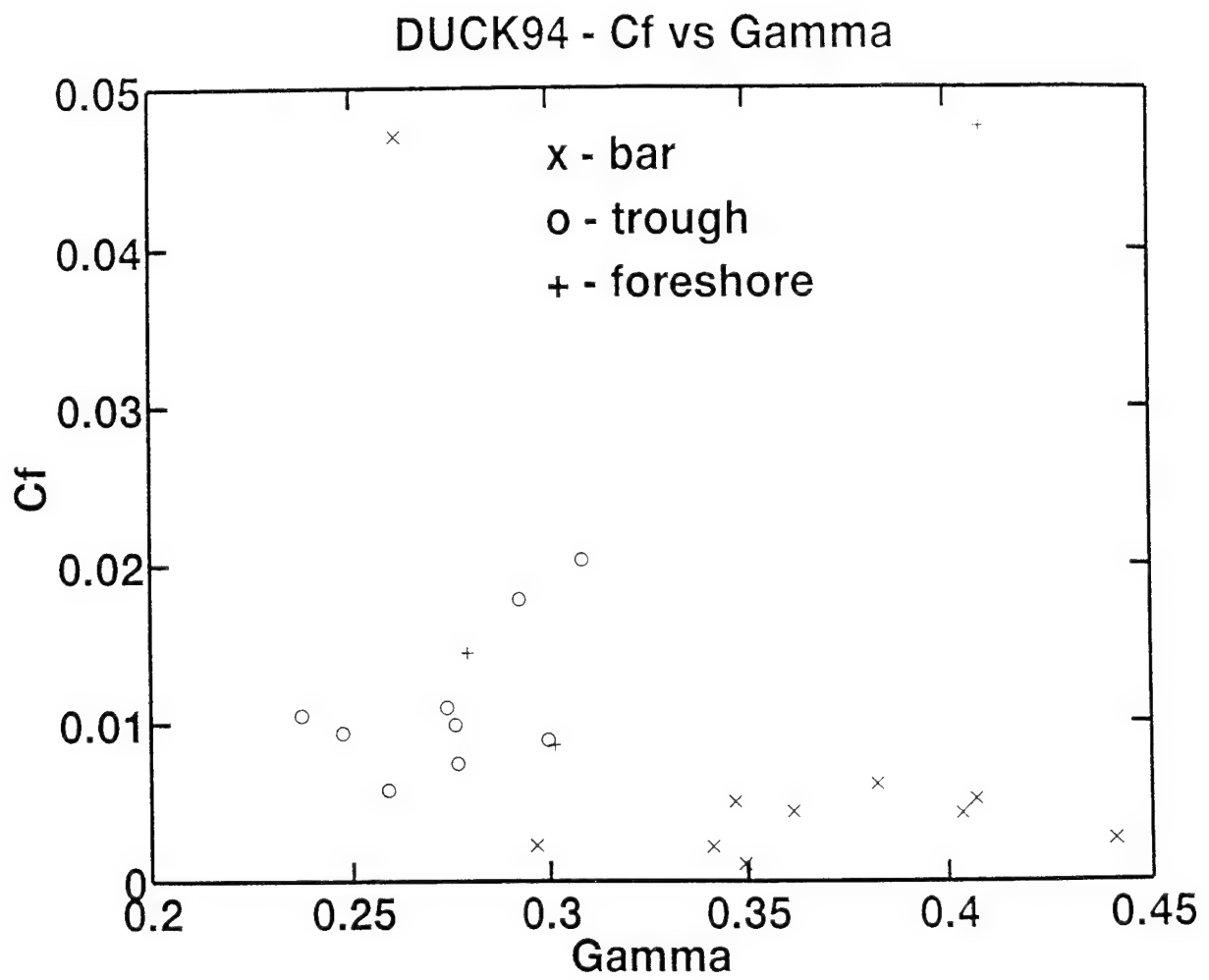


Figure 16. Relationship Between  $C_f$  and  $\gamma$

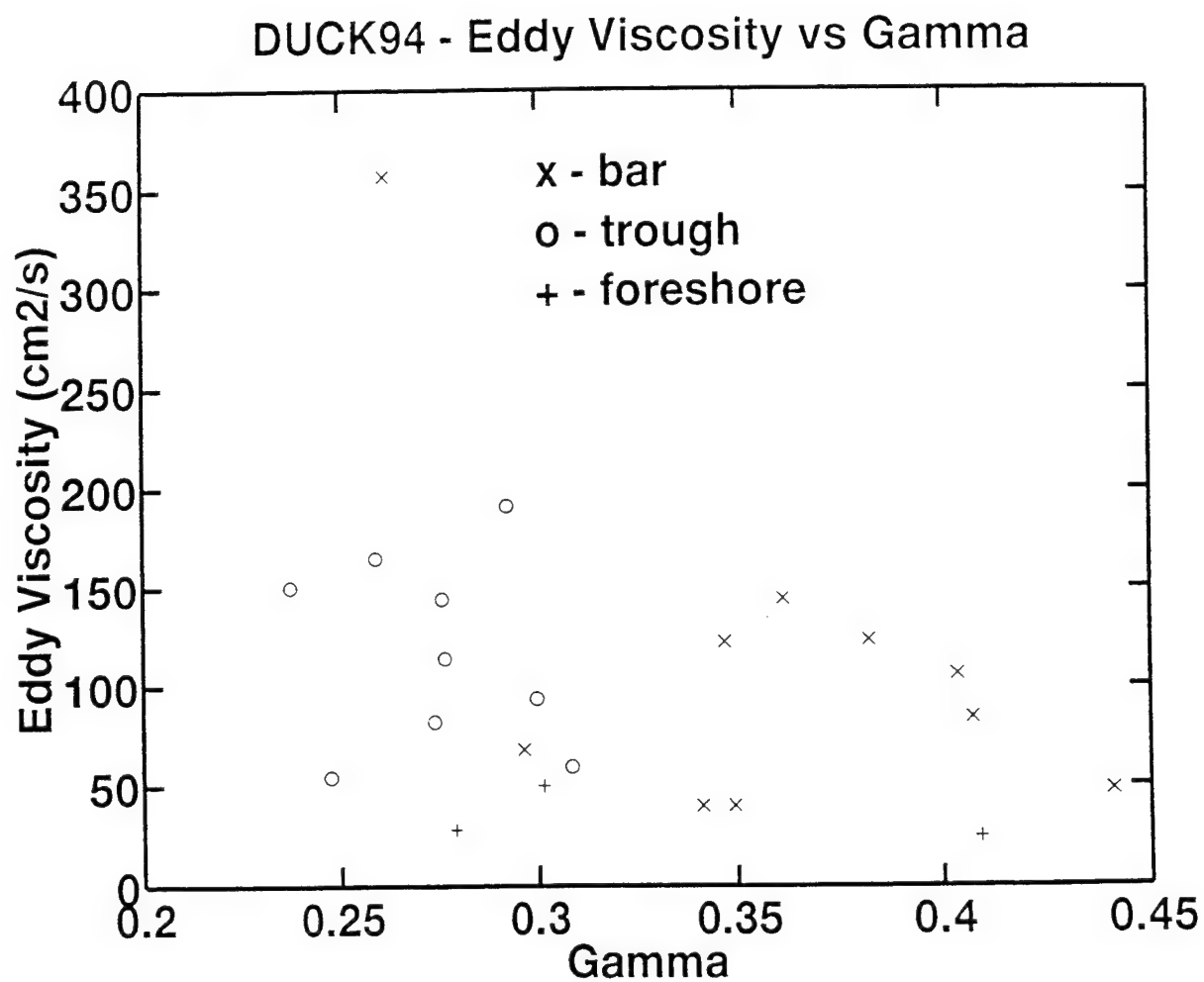


Figure 17. Relationship Between  $v_t$  and  $\gamma$ .

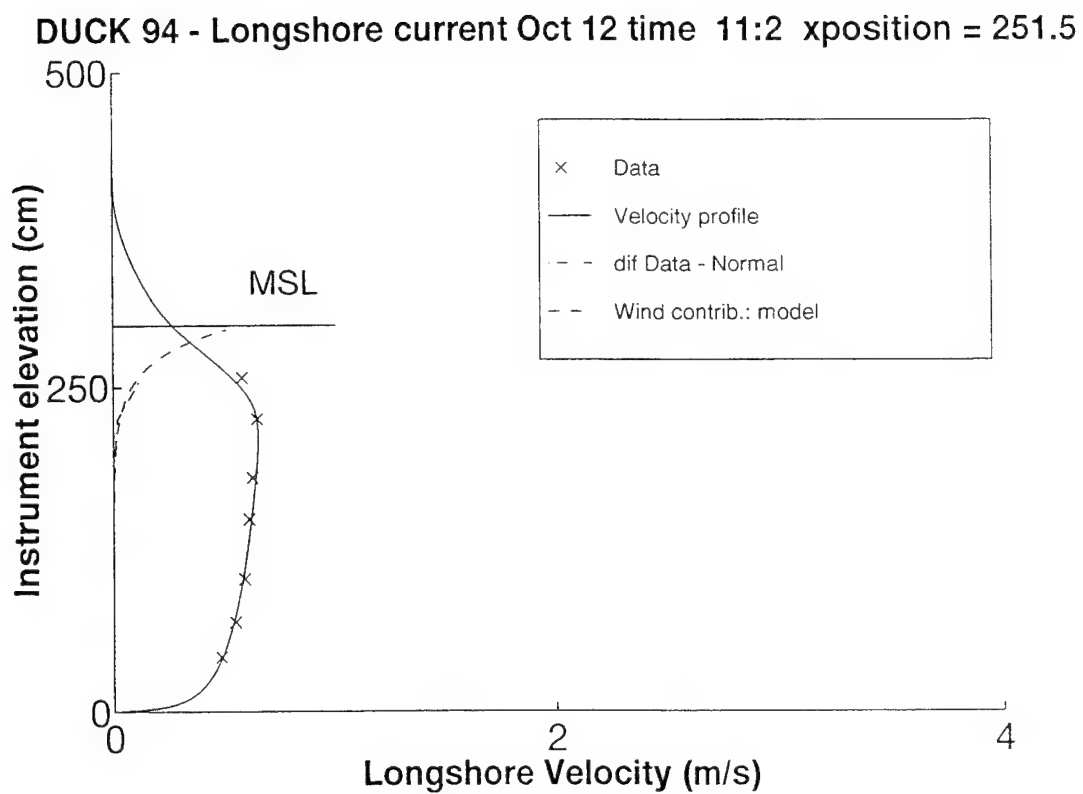


Figure 18. Example of wind contribution to the longshore current: exponential approximation to the residual.

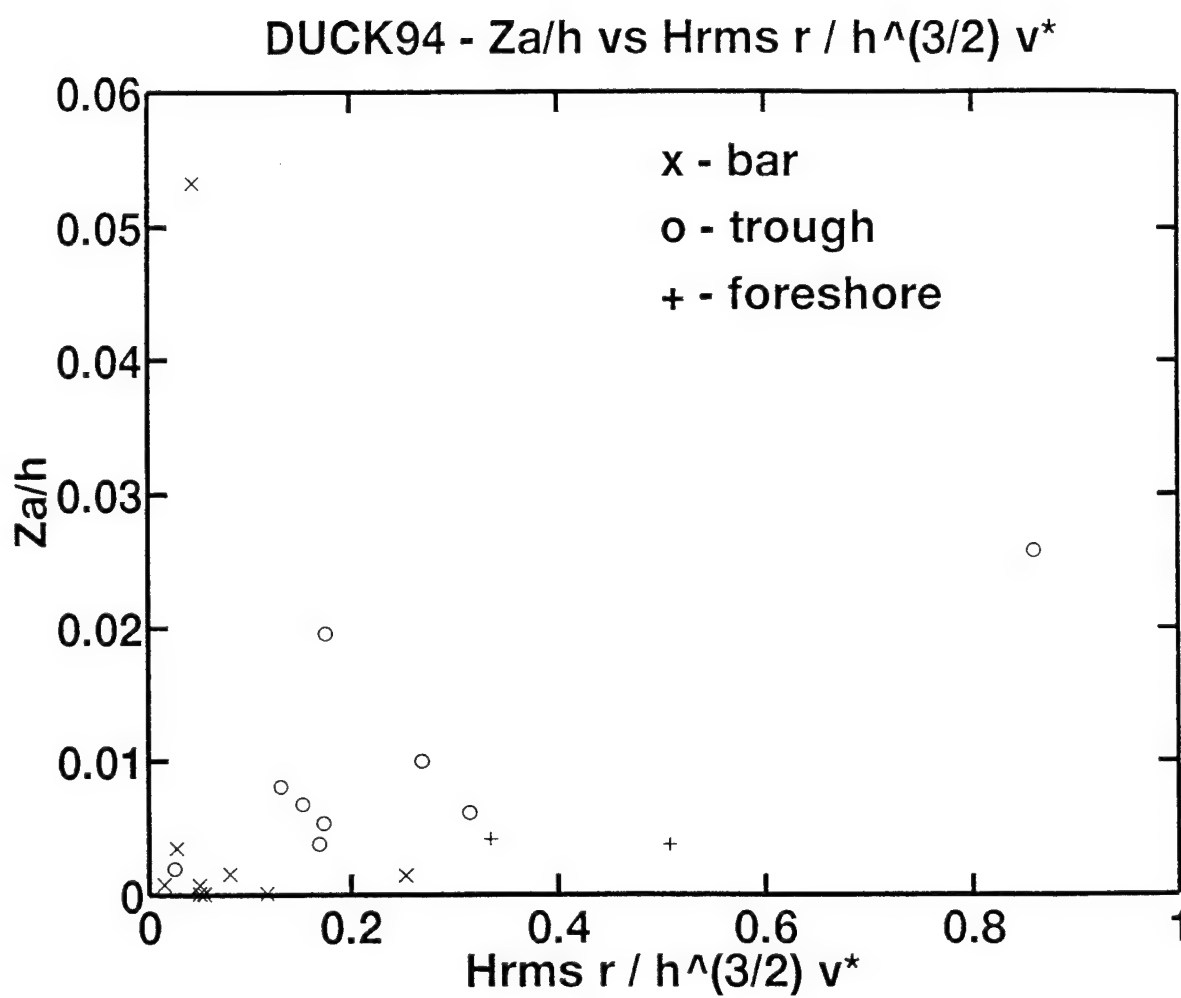


Figure 19. Relationship Between  $\frac{z_a}{h}$  and  $\frac{H_{rms}}{h^{3/2}} \frac{r}{v^*}$ .





## APPENDIX B. TABLES



Run	Time	X-Pos. (m)	h (m)	Hrms (m)	$\gamma$	$z_a$ (cm)	$v_*$ (cm/s)	$C_f$	$v_t$ ( $cm^2/s$ )	corr. coef.
101	7:33	291	3.80	1.11	0.29	0.03	2.70	0.002	68.3	0.98
102	9:06	261	3.24	1.12	0.35	0.01	1.85	0.001	39.9	0.96
103	10:10	231	3.26	1.15	0.35	0.50	5.62	0.005	122.3	0.97
104	12:22	201	3.45	0.89	0.26	0.67	7.18	0.005	165.1	0.99
105	14:06	185	3.18	0.75	0.24	2.57	7.09	0.011	150.4	0.99
106	15:36	170	2.57	0.63	0.25	1.37	3.18	0.009	54.5	0.99
107	16:57	156	1.98	0.55	0.28	0.82	2.13	0.014	28.1	0.99
111	7:53	292	3.66	1.30	0.36	0.28	5.92	0.004	144.3	0.96
112	9:29	270	3.16	1.27	0.40	0.23	5.02	0.004	105.9	0.96
113	10:45	244	3.16	1.12	0.35	1.10	5.85	0.006	127.4	0.97
114	12:01	230	3.75	0.98	0.26	19.98	14.28	0.047	357.4	0.91
115	13:17	187	3.24	0.89	0.27	1.23	5.29	0.007	114.4	0.99
116	14:30	171	3.05	0.84	0.28	3.05	4.05	0.011	82.3	0.99
117	15:44	157	2.50	0.76	0.30	0.93	3.01	0.009	50.1	0.99
118	17:03	146	1.63	0.66	0.40	3.23	2.25	0.048	24.4	0.89
121	7:44	298	3.51	1.23	0.35	0.03	1.70	0.002	39.9	0.97
122	9:27	273	2.93	1.30	0.44	0.03	2.44	0.003	47.7	0.93
123	11:02	252	2.98	1.21	0.41	0.43	4.23	0.005	84.1	0.99
124	12:26	225	3.54	1.04	0.29	6.93	8.11	0.018	191.5	0.99
125	13:26	210	3.51	0.97	0.28	2.37	6.17	0.010	144.5	0.99
126	15:13	188	2.99	0.90	0.30	1.83	4.72	0.009	94.0	0.99
127	16:22	172	2.74	0.84	0.31	7.05	3.26	0.020	59.6	0.98

**Table 1.** Profile Fitting Results.

Run	Time	Cross-Shore Position (m)	Wind speed (m/s)	Wind Current angle(°)
101	7:33	291	12.2	23
102	9:06	261	12.1	16
103	10:10	231	12.9	19
104	12:22	201	11.7	15
105	14:06	185	11.4	11
106	15:36	170	11.6	9
107	16:57	156	11.2	12
111	7:53	292	12.3	44
112	9:29	270	11.8	40
113	10:45	244	10.9	39
114	12:01	230	11.0	39
115	13:17	187	11.1	35
116	14:30	171	11.3	40
117	15:44	157	10.6	41
118	17:03	146	11.0	41
121	7:44	298	14.1	56
122	9:27	273	14.3	56
123	11:02	252	13.5	55
124	12:26	225	14.1	57
125	13:26	210	13.9	59
126	15:13	188	13.9	59
127	16:22	172	13.8	58

**Table 2.** Wind Data

## REFERENCES

- Christoffersen, J.B. and Jonsson, I.G., 1985. Bed friction and dissipation in a combined current and wave motion. *Ocean Engineering*, 12(5): 387-423.
- Church, J.C., 1993. Topics in Longshore currents. Ph.D. dissertation. Naval Postgraduate School, Monterey.
- Church, J.C. and Thornton, E.B., 1993. Effects of breaking wave induced turbulence within a longshore current model. *Coastal Engineering*, 20: 1-28.
- Deigaard, R., Fredsoe, J. And Hedegaard, I.B., 1986. Suspended sediment in the surf zone. *J. Waterway, Port, Coastal and Ocean Engineering*, ASCE, 112(1):115-128.
- Grant, W.D. and Madsen, O.S., 1979. Combined wave and current interaction with a rough bottom. *Journal of Geophysical Research*, 84(C4):1797-1808.
- Murray, S.P., 1975. Trajectories and speeds of wind-driven currents near the coast. *Journal of Physical Oceanography*, 5: 347-360.
- Myrhaug, D. And Slaattelid, O., 1989. Combined wave and current boundary layer model for fixed rough seabeds. *Ocean Engineering*, 16(2):119-142.
- Nielsen, P., 1992. Coastal bottom boundary layers and sediment transport. 324 pp. *World Scientific*, Singapore.
- Roelvink, J. And Reniers, A., 1994. Upgrading of a quasi-3D hydrodynamic model.
- Philips, O.M., 1977. The dynamics of the upper ocean. *Cambridge University Press*, NY, 2nd edition, 316 pp.
- Simons, R.R., Grass, T.J. and Mansour-Tehrani, M., 1992. Bottom shear stresses in the boundary layers under waves and currents crossing at right angles. In: *Proceedings 23th Coastal Engineering Conference, ASCE*, pp. 604-617.
- Sleath, J.F.A., 1990. Velocities and bed friction in combined flows. In: *Proceedings 22th Coastal Engineering Conference, ASCE*, pp. 450-463.
- Swayne, J., 1995. Small-scale morphology during DUCK94. M.S. thesis, Naval Postgraduate School, Monterey, CA.

Visser, P.J., 1984. Uniform longshore current measurements and calculations. In: *Proceedings 19th Coastal Engineering Conference, ASCE*, pp. 2192-2207.

Visser, P.J., 1986. Wave basin experiments on bottom friction due to current and waves. In: *Proceedings 20th Coastal Engineering Conference, ASCE*, pp. 807-821.

Whitford, D.J., 1988. Wind and wave forcing of longshore currents across a barred beach. Ph.D. dissertation. Naval Postgraduate School, Monterey.

Whitford, D.J. and Thornton, E.B., 1993. Comparison of wind and wave forcing of longshore currents. *Continental Shelf Research*, 13(11): 1205-1218.

## INITIAL DISTRIBUTION LIST

		Number of copies
1.	Defense Technical Information Center Cameron Station Alexandria, VA 22304-6145	2
2.	Library Code 52 Naval Postgraduate School 411 Dyer Rd. Rm. 104 Monterey, CA 93943-5101	2
3.	Oceanography Department Code OC/Co Naval Postgraduate School 833 Dyer Rd. Rm. 331 Monterey, CA 93943	1
4.	Prof E.B. Thornton Oceanography Department Code OC/Tm Naval Postgraduate School 833 Dyer Rd. Rm. 331 Monterey, CA 93943	2
5.	Prof. T. Stanton Oceanography Department Code OC/Tm Naval Postgraduate School 833 Dyer Rd. Rm. 331 Monterey, CA 93943	2
6.	LT Carlos Ventura Soares Instituto Hidrografico Rua das Trinas, 49 1296 Lisboa Codex Portugal	2

- |     |                                                                                                                                           |   |
|-----|-------------------------------------------------------------------------------------------------------------------------------------------|---|
| 7.  | Instituto Hidrografico<br>Escola de Hidrografia e<br>Oceanografia<br>Rua das Trinas, 49<br>1296 Lisboa Codex<br>Portugal                  | 3 |
| 8.  | LCDR Manuel Abreu<br>Divisao de<br>Cartografia Nautica<br>Instituto Hidrografico<br>Rua das Trinas, 49<br>1296 Lisboa Codex<br>Portugal   | 1 |
| 9.  | LCDR Seabra de Melo<br>Divisao de<br>Oceanografia Fisica<br>Instituto Hidrografico<br>Rua das Trinas, 49<br>1296 Lisboa Codex<br>Portugal | 1 |
| 10. | Prof. T. Lippmann<br>Scripps Institution of Oceanography<br>La Jolla, CA 92037                                                            | 1 |
| 11. | Commander<br>Naval Oceanography Command<br>Stennis Space Center, MS 39529-5000                                                            | 1 |
| 12. | Commanding Officer<br>Naval Oceanographic Office<br>Stennis Space Center, MS 39529-5001                                                   | 1 |
| 13. | Superintendent<br>Naval Research Laboratory<br>Marine Geosciences Div Code 7400<br>Stennis Space Center, MS 39529-5000                    | 1 |
| 14. | Chief of Naval Research<br>800 N. Quincy Street<br>Arlington, VA 22217                                                                    | 1 |



- |     |                                                                                                                                             |   |
|-----|---------------------------------------------------------------------------------------------------------------------------------------------|---|
| 15. | Office of Naval Research<br>Ocean Sciences Directorate (Code 1121 CS)<br>Attn: Thomas Kinder<br>800 N. Quincy Street<br>Arlington, VA 22217 | 1 |
| 16. | Dr. Dennis Whitford<br>Chairman<br>Oceanography Department<br>U.S. Naval Academy<br>Annapolis, MD 21402                                     | 1 |
| 17. | Library<br>Scripps Institution of Oceanography<br>La Jolla, CA 92037                                                                        | 1 |
| 18. | Director<br>U.S. Army Coastal Engineering Research Center<br>Kingman Building<br>Ft. Belvoir, VA 22060                                      | 1 |
| 19. | Director<br>Waterways Experiment Station<br>Corps of Engineers<br>3909 Hall's Ferry Rd<br>Vicksburg, MS 39180-6199                          | 1 |